

THE TRANSIENT PROCESS OF ESTABLISHING A  
STEADILY ALTERNATING CURRENT ON A LONG  
LINE, FROM LABORATORY MEASURE-  
MENTS ON AN ARTIFICIAL LINE.

BY A. E. KENNELLY AND U. NABESHIMA.

(Read April 22, 1920.)

The purpose of this paper is to make a contribution to the theory, records and measurement technique of transient electromagnetic wave propagation over long uniform conductors, with particular reference to the upbuilding of the alternating-current steady state over long alternating-current power-transmission lines, from measurements made on artificial power-transmission lines in the laboratory.

As is shown in the appended bibliography, the subject has been already developed to a considerable extent from the theoretical side. Very little, however, seems to have been published on the practical side. The research here described has been mainly directed to the practical side of the subject, from the laboratory viewpoint. It was taken up in October, 1917, in thesis work towards a master's degree.<sup>1</sup> It was later continued from May, 1919, to the present date, as a research in the electrical Research Division at the Massachusetts Institute of Technology.

*Classification of Transients.*—For the purposes of discussion and analysis, it is desirable to establish certain provisional definitions relating to transient electromagnetic phenomena, in order to avoid ambiguity.

A transient may be defined as a temporary and evanescent disturbance in an electric circuit, or in the indications of apparatus connected therewith, due to any arbitrary sudden change imposed

<sup>1</sup> Bibliography 36.

upon the circuit. A permanent or steady electromagnetic state cannot therefore contain transients to any appreciable extent; although transients will probably have been involved in the production of that state. It is true that transient phenomena persist with progressive attenuation for an indefinitely long period, and, in that sense, never completely disappear. From an engineering point of view, however, transients diminish into practical negligibility in a period of time that is ordinarily measured in milliseconds; so that they may be regarded as having vanished, when the steady state is accepted as having been attained.

For the purposes of discussion, transients are subdivided as shown in Table I.

Class *A* includes transients of all kinds, mechanical and electrical. Thus, a kick of the pen of a recording ammeter pointer might represent a mechanical transient due to an electrical transient.

Prominent among transients are electromagnetic-wave transient disturbances, or *wave transients*.

An important class of wave transients are those which accompany the establishment of an alternating current over a line. These may be classed collectively as initiating *a.-c. transients*. This is the principal class of transients discussed in this paper.

Initiating alternating-current wave transients occur, in general, whenever a switch is closed at the generating end of an *a.-c.* line. If the switch could be closed in such a manner as to produce no electric "splash," the outgoing wave transient would be the "regular" transient, which accompanies the regular formation of the final alternating-current state.

*Infinite Distortionless Line Closed at Zero E.m.f. (No Transients).*—If we assume, for simplicity, a perfectly regulated sine-wave generator, of negligible internal impedance, connected as in Fig. 1 to an indefinitely long uniform distortionless line,<sup>2</sup> then if the switch *S* is closed at some instant when the alternating e.m.f. is passing through zero, the initial outgoing waves of e.m.f. and cur-

<sup>2</sup> A distortionless line was originally defined by Heaviside as a line in which  $l/r = c/g$ . In such a line, the surge impedance  $z_0$  must have zero slope at all frequencies, or becomes reactanceless. See Bibliography (1), page 126, Vol. II.; also Bibliography (30), page 154.



rent will be splashless; *i.e.*, they will be sinusoidal and in cophase from the very start. In such a case, because there can be no reflection from the distant end, the initial outgoing current will be the same, both as to magnitude and phase, as the final outgoing

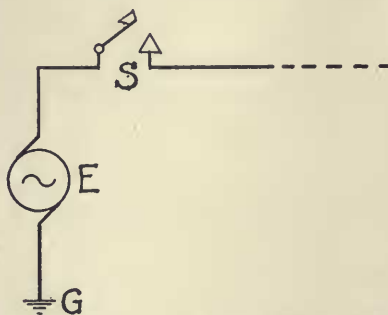


FIG. 1. Diagram of A. C. Generator Connected to Line.

current; or there will be no transient wave. In this particular and simple case, if  $z_0$  is the reactanceless surge impedance of the line, in ohms,  $E_A$  the maximum cyclic e.m.f. in vector volts at standard phase, the initial and final outgoing current will be

$$I_0 = \frac{E_A}{z_0}, \quad \text{max. cyc. amperes } \angle. \quad (1)$$

If the frequency of the impressed e.m.f. is  $f$  cycles per second, and the corresponding angular velocity  $\omega = 2\pi f$  radians per second, then, at time  $t$  seconds after the switch closure, the instantaneous voltage and current at  $A$  will be

$$e = E_A \sin \omega t \quad \text{instantaneous volts,} \quad (2)$$

$$i = \frac{E_A}{z_0} \sin \omega t \quad \text{instantaneous amperes.} \quad (3)$$

Because of the simple conditions assumed in this case, including infinite line length, the current defined by (3) is instantly developed without the intervention of any transient. If the line has finite length, but is grounded at  $B$  through an impedance equal to the surge impedance  $z_0$ , it will give rise to no reflections from  $B$ , and will behave, in this respect, like a line of infinite length. Such a case is represented in Fig. 12 (film 35).

*Finite Smooth Distortionless Line closed at Zero E.m.f. (Regular Transients).*—If, instead of assuming an infinite line, or its equivalent—a line of finite length  $AB$ , grounded at  $B$  through a resistance equal to the surge resistance  $z_0$ —we apply the above stated conditions to a finite smooth line, grounded at  $B$  through some other impedance, reflected waves of voltage and current will return to the generating end  $A$ , and will add themselves to the outgoing stream. These successive increments build up regularly into the steady state, at each and every point along the line.<sup>3</sup> The initial outgoing e.m.f. and current are therefore transients in this case, as are also all the reflected increments. Such wave transients may therefore be described as “regular” wave transients, because their regular superposition and combination bring about the final steady state.

*Finite Smooth Line, with Distortion, Closed at Zero E.m.f. (Splash Transients).*—If the uniform smooth line  $AB$  is not only finite; but also has distortion, its surge impedance  $z_0$  will contain reactance, and have some angle or slope. In the steadily alternating-current state, therefore, at any point along the line, the current and voltage will not, in general, be in cophase. At an instant of zero current, there will be some e.m.f. and at any instant of zero

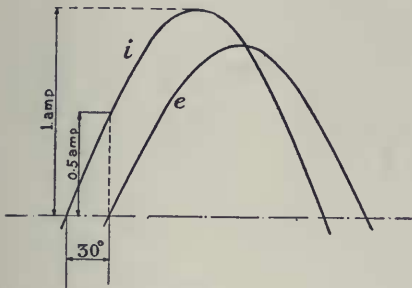


FIG. 2a.

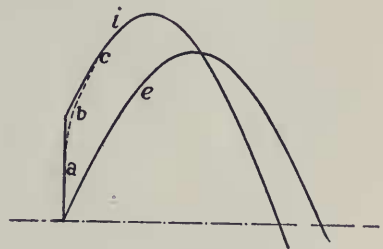


FIG. 2b.

Illustrating formation of a Current Splash Transient.

e.m.f. there will be some current. Consequently, if the switch is closed at an instant of zero e.m.f., there will be some accompanying “electric splash”; because the current is then forced to start from zero coincidentally with the e.m.f. In Fig. 2a, the wave  $i$  of

<sup>3</sup> Bibliography 6, and 13 page 79.

normally outgoing current is represented as leading, by  $30^\circ$ , the associated outgoing wave  $e$  of e.m.f.; so that at an instant of zero e.m.f., the strength of the current will be 0.5 ampere. In Fig. 2*b*, the switch at the generator end of the line is supposed to be closed at an instant of zero e.m.f. The instantaneous outgoing current must also be zero at that moment. The first outgoing half wave of current is therefore distorted from the sinusoidal form, and follows a course such as is indicated approximately by the dotted line *abc*. This distortion gives rise to a splash transient.

A splash wave transient may therefore be defined as that transient wave disturbance which is due either to closing the line switch at a moment when the generator e.m.f. is off zero; or, if the generator e.m.f. is zero, to the zero of line current forced at that instant, when the surge impedance of the line calls for a definite phase difference between outgoing current and voltage. In general, the splash transient will be greater, the greater the value of the impressed e.m.f. at switch closure. The splash can only be zero in the case of a distortionless line closed at an instant of zero e.m.f. It may, however, be expected to be a minimum, on any ordinary line, when closed at or near an instant of zero e.m.f.; because if there is no e.m.f. splash, the current splash is usually very small.

*Lumpy Artificial Line Closed at Zero E.M.F. Lumpiness Transients.*—If an artificial line, made up of alternate coils and condensers, is used in place of a smooth and uniform line; the lumpiness of the line will give rise to another type of transient,<sup>4</sup> which may be called a "lumpiness" transient. This lumpiness transient may be regarded as being produced by oscillatory disturbances between the successive coils and condensers. Lumpiness transients are magnified by the sudden application of a large e.m.f. In other words, the conditions which produce splash transients on smooth lines are also those which favor lumpiness transients on artificial lines. In laboratory measurements of lumpy artificial lines, lumpiness transients must therefore be expected over and above the transients due to splash.

Table I. presents a provisional classification of transients con-

<sup>4</sup> Bibliography 37.

nected with electric circuits. These may be divided into subclasses in a variety of ways. The transients particularly discussed in this paper are the regular transients  $M$ , which are a branch of the initiating  $a$ - $c$ . wave transients, and which belong to the principal class  $A$  through subdivisions  $E$ ,  $F$ ,  $H$ , and  $J$ .

*Artificial Line Employed.*—The measurements reported in this paper were all carried out on an artificial line in the electric transmission laboratory of the Massachusetts Institute of Technology. This is an artificial power-transmission line of 26  $\pi$ -sections, designed by Drs. Pender and Huxley, the construction and dimensions of which have been described elsewhere.<sup>5</sup> It represents an aerial singlephase copper conductor of 253 sq. mm. (500,000 cir. mils) cross section, using ground or neutral return, and having the constants given in the following table.

TABLE II.

## PARTICULARS OF THE ARTIFICIAL LINE CHIEFLY USED IN TESTS.

|   |                |           |
|---|----------------|-----------|
| Length of Conjugate Smooth Line per section | .....48.28 km. | 30 miles  |
| Total of 26 sections                        | ..... 1255 km. | 780 miles |

|   | Whole Line.            | Per Section.            |
|---|------------------------|-------------------------|
| Conductor Res: $R$ at 19° C., ohms          | 87.71                  | 3.374                   |
| Inductance $L$ , henrys                     | 1.457                  | 0.05605                 |
| Reactance $X$ , at 60.6~, ohms              | 555                    | 21.345                  |
| Dielectric Leakance $G$ , mhos              | $15.14 \times 10^{-6}$ | $0.5823 \times 10^{-6}$ |
| Dielectric Capacitance $C$ , farads         | $12.58 \times 10^{-6}$ | $0.4838 \times 10^{-6}$ |
| Dielectric Susceptance $B$ , at 60.6~, mhos | $4.790 \times 10^{-3}$ | $0.1842 \times 10^{-3}$ |

| Linear Constants.                       | Per Wire Km.            | Per Wire Mile.          |
|---|-------------------------|-------------------------|
| Linear Resistance $r$ at 19° C., ohms   | 0.06987                 | 0.11245                 |
| Linear Inductance $l$ , henrys          | $1.1611 \times 10^{-3}$ | $1.8683 \times 10^{-3}$ |
| Linear Reactance $x$ , at 60.6~, ohms   | 0.4421                  | 0.7115                  |
| Linear Leakance $g$ , mhos              | $1.206 \times 10^{-8}$  | $1.941 \times 10^{-8}$  |
| Linear Capacitance $c$ , farads         | $1.002 \times 10^{-8}$  | $1.6127 \times 10^{-8}$ |
| Linear Susceptance $b$ , at 60.6~, mhos | $3.816 \times 10^{-6}$  | $6.141 \times 10^{-6}$  |

Surge Impedance  $z_0$  of line, or of a section, at 60.6~,  $342.5 \nabla 4^\circ 24'$  ohms  $\angle$

Angle  $\Theta$  subtended by whole line, at 60.6~,

$$1.6405 \angle 85^\circ 25' 8'' = 0.1315 + j 1.6352 = 0.1315 + j 1.041 \text{ hyps } \angle.$$

Angle  $\theta$  subtended by single section, at 60.6~,

<sup>5</sup> Bibliography 17a and 30.

$$0.0631 \angle 85^\circ 25' 8'' = (5.058 + j 40.04) 10^{-3} \text{ hyps } \angle.$$

Linear angle  $\alpha$  at 60.6 ~,

$$1.307 \times 10^{-3} \angle 85^\circ 25' 8'' = (0.1048 + j 1.302) 10^{-3} \\ = (0.1048 + j 0.8293) 10^{-3} \text{ hyp/km.}$$

Linear angle  $\alpha$  at 60.6 ~,

$$2.103 \times 10^{-3} \angle 85^\circ 25' 8'' = (0.1686 + j 2.096) 10^{-3} \\ = (0.1686 + j 1.335) 10^{-3} \text{ hyp/mile.}$$

Lumpiness correction of line, or of any section, in steady state, at 60.6 ~,

$$\frac{\theta}{a} / \sinh \frac{\theta}{a} = 1.0002 \angle 0^\circ.0002.$$

The lumpiness correction factor of this line in the steady state is  $1.0002 \angle 0^\circ.0002$  at 60 ~, which, for practical purposes, is quite insignificant. This means that, for a.-c. transmission in the steady state, at 60 ~, this lumpy artificial line is equivalent to the smooth uniform line having the linear constants  $r$ ,  $g$ ,  $l$  and  $c$  of Table II. At 189.4 ~, however, the lumpiness correction factor, in the steady state, is  $1.002 \angle 0^\circ.01$ , and at yet higher frequencies, it becomes very appreciable. A picture of part of this line appears in Fig. 8.

In most of the measurements of transients made on this line, the full length of 26 sections, 1255 km., or 780 miles, was employed. At 60.6 ~—the frequency ordinarily used—this length is nearly a quarter wavelength,<sup>6</sup> so that, in the steady state, with the distant end  $B$  free, the voltage at  $B$  with the oscillograph connected there, rises to  $5.627 \angle 110^\circ.6$  times the voltage impressed at  $A$ .

*Electrical Connections.*—The electrical connections most frequently employed in the tests are indicated in Fig. 3.  $AB$  is the

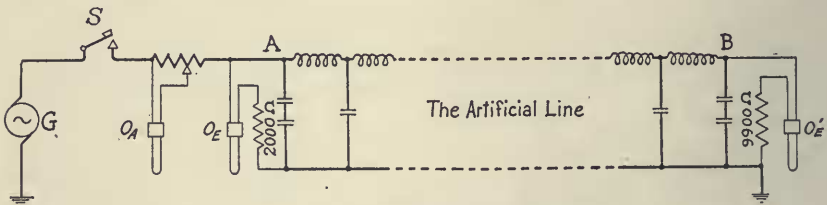


FIG. 3. Electrical Connections of Artificial Line.

artificial  $\pi$  line. At the generator end  $A$ , is a single-pole motor-controlled line switch  $S$ , for closing the circuit at any desired phase of e.m.f. from the alternator  $G$ . A current-recording oscillograph

<sup>6</sup> Bibliography 13, p. 82.



$O_A$  records the initial current waves entering the line for the first few cycles after the switch  $S$  is closed. The voltage-recording oscillograph  $O_E$  records simultaneously the wave form of the impressed e.m.f. The distant or receiving end  $B$ , is freed in Fig. 3, except that it is connected to ground through the high non-inductive resistance, ordinarily of 9900 ohms, in order to permit of operating the voltage-recording oscillograph  $O_E'$ . All three oscillographs are set into operation simultaneously, on closing the phase-selecting switch  $S$ , during about 8 cycles from the  $60\sim$  generator  $G$ , or for a duration of about  $\frac{2}{15}$  second; and all three are recorded on the same photographic film 8.25 cm. ( $3\frac{1}{4}$  inches) wide. In this manner, the voltage at each end of the line, and the current at the entering end, are recorded immediately after closing the line switch  $S$ .

*Alternating-Current Generator.*—The a.-c. generator  $G$ , Fig. 3, was a 6-pole 10-k.v.a. alternator of the Lauffen type, designed by Prof. C. A. Adams, for the delivery of a nearly pure sine-wave e.m.f. At the time these tests were made, no other load was connected to the machine. It was driven by a directly coupled d.-c. 110-volt motor, of approximately 10 kw. continuous rating, rotating at approximately 1200 r.p.m. The current in the d.-c. motor field magnet was adjusted in the testing room, so as to maintain constant frequency. The frequency was measured in the testing room by mounting a stroboscopic disk on the shaft of the small synchronous motor, and observing this revolving disk, illuminated by a fixed incandescent lamp, through slits in the prongs of a stroboscopic<sup>7</sup> fork on a telescope. Unless in such measurement, the frequency is held constant, the results are of little value.

*Oscillograph.*—The oscillograph had three vibrators, in an electromagnetic field common to all. The instrument was designed and constructed by Mr. H. G. Crane, at Harvard University. The bifilar vibrators had a working length of 12.5 mm., and were damped in castor oil. As the currents observed were of low frequency, the correction factors for frequency of the vibrators<sup>8</sup> are insignificant at  $60\sim$ , and are omitted.

<sup>7</sup> Bibliography 7.

<sup>8</sup> Bibliography 39.

Ammeters and voltmeters of the alternating-current type were introduced, at special times, into the artificial-line circuits, in order to secure calibrations of the oscillograms. The impressed e.m.f. at *A* ranged, in different cases, from 60 to 100 volts r.m.s.

*Line-Switch Connections.*—In order to minimize splash transients, it was necessary to design and make up a switch, which would connect the 60 ~ alternator to the artificial line at an instant of zero e.m.f. For this purpose, a little 6-pole synchronous motor, running in synchronism with the a.-c. generator, was caused to drive an insulating disk *D*, Fig. 4, carrying a 60° conducting sector

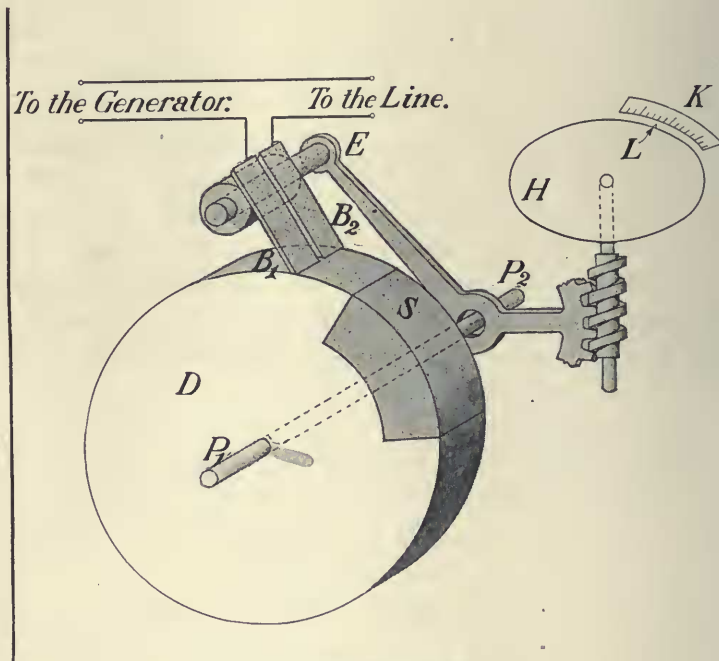


FIG. 4. Brush Mechanism.

*S*, in such a manner that a pair of insulated brushes  $B_1B_2$ , resting thereon, could be brought into contact, through the sector, at any desired position around its circumference. The final adjustment of phase position was secured by means of the graduated pointer and scale *LK*, divided into single degrees of arc. One electrical degree

of phase shift corresponds to  $24^\circ$  of  $LK$  mechanical-arc adjustment. This adjustment is also illustrated in Fig. 5, where the pointer  $P$

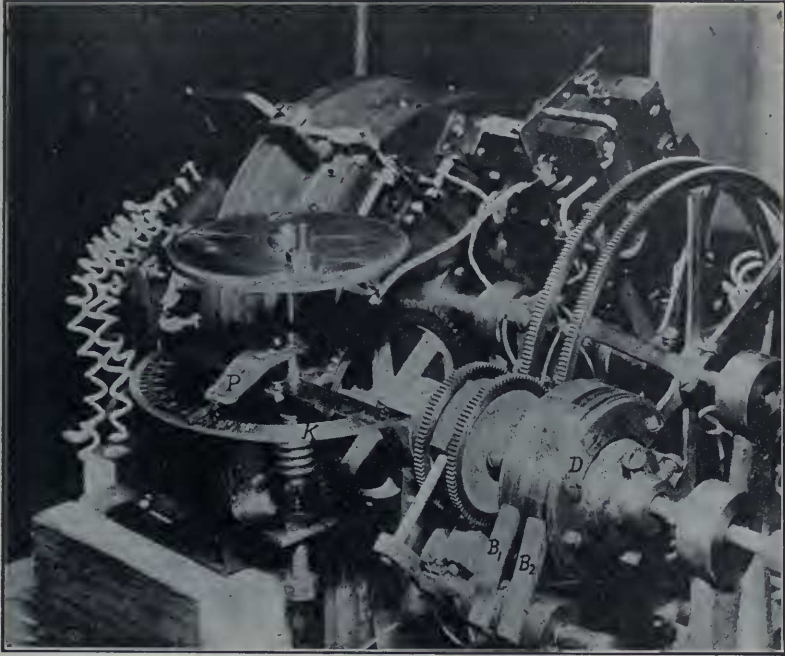


FIG. 5. Time-controlling Mechanism of Circuit-closing Switch.

stands over the stationary scale  $K$ , and determines the position of the brushes  $B_1B_2$  around the sectored insulating disk  $D$ . One electrical degree of a  $60 \sim$  alternator corresponds to  $\frac{1}{21600}$  of a second,

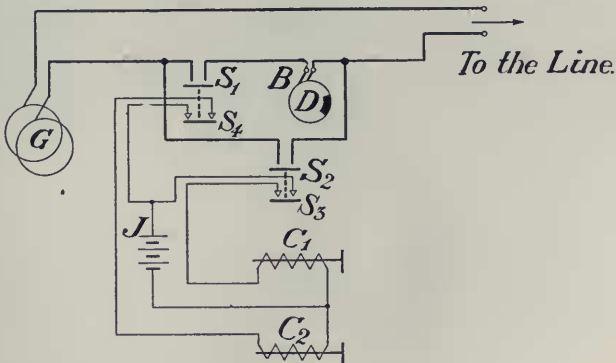


FIG. 6. Switch Diagram.

or 46.3 microseconds, so that, theoretically, 1 degree of arc in the setting of the pointer  $P$  corresponds approximately to 2 microseconds of time.

*Technique of Making Records.*—The electrical connections of the switch mechanism are indicated in outline by Fig. 6. The alternating-current generator  $G$ , is supposed to be in regular operation at the correct frequency. The above mentioned synchronous motor, shown in plan view in Fig. 7, is then started, and synchron-

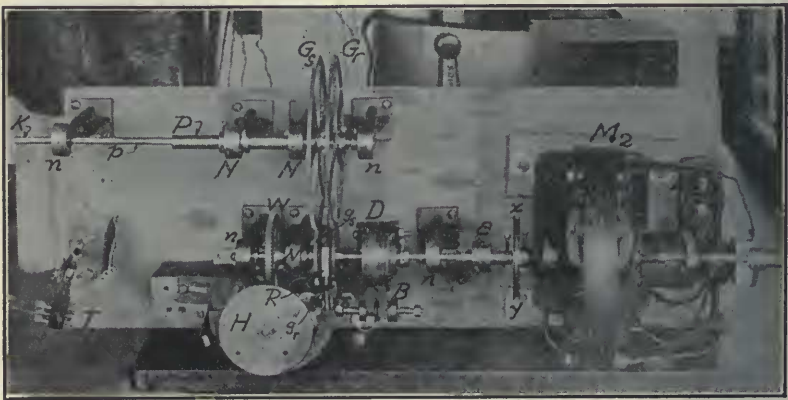


FIG. 7. Plan View of Synchronous Motor and Circuit-closing Switch.

ized with the generator. The arc lamp for the oscillograph vibrators is then lit. The brushes  $B_1B_2$ , Fig. 4, are next set in the correct position to close the generator on the artificial line at an instant of zero e.m.f. This adjustment is made by trial, substituting a simple non-inductive resistance for the artificial line, and closing the generator through the brushes, and an oscillograph, so as to observe on the translucent screen whether the beam of light starts into vibration without a splash. The setting of the brushes to effect this result can usually be adjusted, with ordinary optical conditions, within one electrical degree, or 46 microseconds for a 60~ generator. The artificial line is then reconnected to the apparatus, all ready for the photographic record. A starting lever is moved by hand, and this causes automatic switch  $S_1$  to be closed, ahead of the rotary switch  $D$ . The brushes  $B_1B_2$  then close the circuit finally,

at the proper predetermined phase of minimum splash. The automatic switch  $S_2$  then immediately follows, so as to keep the contact closed on the line after the brushes  $B_1B_2$  have passed off the contact segment. Before the brushes  $B_1B_2$  close, the photographic shutter is opened by the electromagnet  $C_1$ , under the action of an automatic switch  $S_3$ . After one complete revolution of the photographic-film drum, another shutter is closed by the electromagnet  $C_2$ , under the control of an auxiliary automatic switch  $S_4$ . This cuts off the arc light from the recording film, after about nine cycles have been recorded on all three oscillographs. The whole mechanism can then be arrested, by hand, at leisure. Lastly, the photographic drum is removed and taken to the dark room for development.

A photographic view of the artificial line and the oscillographic apparatus is shown in Fig. 8.



FIG. 8. Artificial Power Transmission Line, Oscillograph and Switching Apparatus.

*Case of Regular Transients.*—About 150 different triple oscillograms have been secured of initial electromagnetic wave transients, under various conditions, over artificial lines. Only a few of these can be dealt with in this paper.

Fig. 9 (Film No. 40) shows the regular transient case for thirteen half cycles on the full-length artificial line, as defined in Table

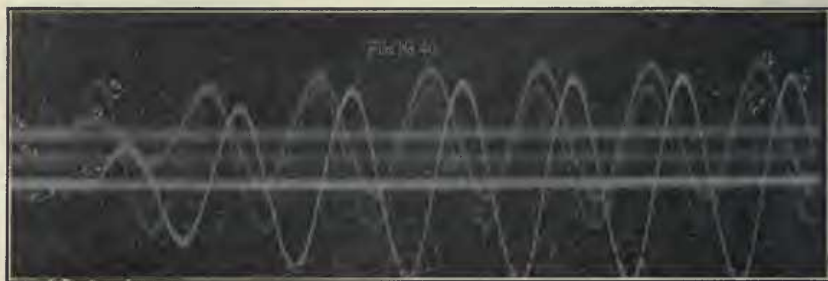


FIG. 9. Triple Oscillogram of  $e_s$ ,  $i_s$  and  $e_r$  for 1255 km. artificial power line freed at distant end.  $f=60.6 \sim$ .

II., at the frequency of  $60.6 \sim$ , with the distant end free (through the oscillograph at  $B$ ), and with the line switch closed at or very near to an instant of zero e.m.f. The electrical connections are those of Fig. 3.

The three curves on Film No. 40, Fig. 9, are  $e_s$ ,  $i_s$  and  $e_r$ , representing respectively the sending-end e.m.f., the sending-end current and the receiving-end voltage. The sending-end voltage (76.7 volts r.m.s.) is seen to be substantially uniform throughout the seven cycles. It may be observed, however, that during the first two or three alterations, the maxima of impressed e.m.f. are slightly higher than those at later stages. This may have been an effect of throwing on the load. The same effect could also be detected on a voltmeter, when throwing the line on and off. In the computations to be subsequently described, these deviations from uniformity in  $e_s$  were taken into account. In the analysis of the oscillographic record, the measured values are all referred, for convenience, to those which, by simple proportion, would be obtained with 100 volts impressed e.m.f.

The  $i_s$  curve starts, without appreciable splash, practically in phase with the e.m.f. Near the end of the first alternation, it is reinforced by a current wave reflection from the distant free end. These reflections keep coming in, approximately in step with the outgoing alternations, so that the final sending-end current is nearly

six times (5.691) the initial sending-end current. This represents a series of regular initiating a.-c. wave transients.

The  $e_r$  curve starts about half an alternation behind the  $e_s$  and  $i_s$  curves, since 4.3 milliseconds are required to transmit the wave along the artificial line, and an alternation at 60.6  $\sim$  lasts 8.25 milliseconds. It then develops into a sinusoidal wave with an amplitude that steadily increases, owing to increments reflected from the sending end. The steady state is, however, very nearly reached by the end of the oscillogram. The ratio of the final to the initial crest value is 5.627. As has been already mentioned, the line happens to be nearly quarter-wave length for the impressed frequency (60.6  $\sim$ ).

The growth of the  $i_s$  curve and especially of the  $e_r$  curve, has been found to be in substantial agreement with the theory of initiating regular transients over the corresponding smooth line, as will shortly be detailed. This means that in spite of the lumpiness of the artificial line, the transient stages of voltage and current development into the a.-c. steady state, are presented substantially as they might be expected over the corresponding smooth line, provided that the voltage application is made at an instant of zero e.m.f.

*Splash and Lumpiness Mingled with Regular Initiating Transient.*—In Fig. 10 (Film 110), the same artificial line,

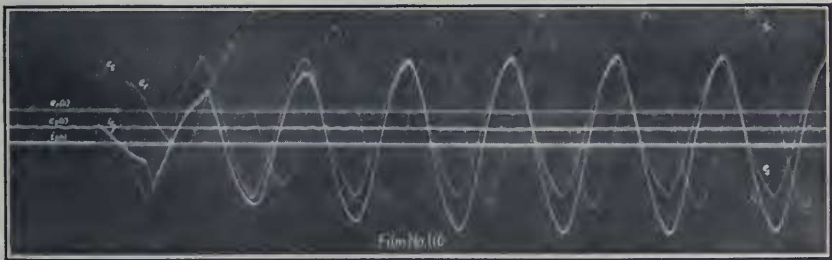


FIG. 10. Example of Splash, Lumpiness and Regular Transients.

freed at the far end, is closed on the same generator at the same frequency. The switch is closed, however, at or near a crest value of impressed e.m.f.  $e_s$ . The entering current  $i_s$ , instead of rising smoothly, as in Fig. 9, jumps up rapidly to crest value, with an

oscillation in the process, and then descends upon a distorted curve. The deviations from the sinusoidal state are clearly visible in  $i_s$  for five alternations, after which the upbuilding progress towards the same final steady state as in Fig. 9, becomes fairly regular. Similarly, the far-end voltage  $e_r$  rises with oscillations which are not attributable to the oscillograph, and are probably lumpiness transients. The deviations from the sinusoidal wave form are visible in the growth of  $e_r$  for at least four alternations. The case is therefore one of mixed splash, lumpiness, and regular initiating transients. The curves of this case have not been analyzed.

The zero line of  $e_s$  contains ripples, which are due to accidental mechanical tremors of the instrument at the moment of zero-line recording. The zero lines were ordinarily recorded after the oscillographic wave records on the line had been secured, and at a time when the instrument was disconnected.

(628 km. or 390 miles) and is grounded at  $B$  through a current-

In Fig. 11 (Film No. 106), the artificial line has half length



FIG. 11. Example of Splash, Lumpiness and Regular Transients.

recording oscillograph. The line switch was set to close at or near a crest of impressed e.m.f. of about 70 volts r.m.s. The splash at  $A$  is very marked, The curve  $i_s$  is the sending-end current, and is very erratic during the first two or three alternations. The receiving-end current  $i_r$  is also very erratic, and contains lumpiness oscillation ripples. It slowly regularises itself, as time goes on, towards the steady state. When the line switch was closed at an instant of zero e.m.f., instead of near the crest value, these erratic waves did not present themselves on this 625 km. line. No attempt has been



made to analyze these curves as yet, owing to the bad splash and lumpiness transients they indicate.

*Splash Transient Occurring Singly.*—If the line is made virtually of infinite length with respect to the sending end, by grounding it at  $B$  through an impedance equal to its surge impedance  $z_0$ , a splash produced by the closing of the line switch off zero e.m.f., will give rise to a splash transient, that will vanish very quickly at  $A$ ; because no reflected waves can return from the distant end. An example of this case is presented in Fig. 12 (Film No. 35).



FIG. 12. Non-recurring Splash and Casual Transients.

Approximately the same half-length artificial line as in Fig. 11 (580 km.), is here grounded at  $B$  through a combination of resistance and condenser, so as to produce an impedance, at 60.6~, of  $342.5 \sphericalangle 4^\circ.4$  ohms. The line switch was closed at a phase of about 20 electrical degrees later than the zero of ascending e.m.f. This is seen to produce a splash both in  $e_s$  and  $i_s$ , the initial outgoing waves of e.m.f. and current. This splash is also seen to be repeated in the  $B$ -end voltage  $e_r$ , where the load ( $z_0$ ) is connected. The splash gives rise also to a lumpiness transient, as may be seen by the ripples in  $i_s$ , the entering current, during the first alternation. A similar lumpiness ripple transient is faintly perceptible in the first alternation of  $e_r$  at  $B$ . Neither splash nor lumpiness transients are visible, however, in the second or succeeding alternations in any of the curves, these disturbances, according to theory, being all absorbed at the  $B$  end, by the load  $z_0$ .

*Casual Transients.*—At the point  $Ae_s$ , Fig. 12, in the fourth

alternation of impressed e.m.f., there is an accidental transient ripple, due to a slip in the contact mechanism of the line-switching apparatus at  $A$ . This momentary disturbance is clearly duplicated simultaneously at  $Ai_s$  in the sending current. After an interval of about 2 milliseconds, a similar ripple transient appears at  $Ae_r$ , in the voltage at  $B$ . All of these transients are absorbed in  $z_0$ , at  $B$ , and do not reappear. Such wave transients may be called *casual transients*, to distinguish them from initiating transients which occur at the starting of an a.-c. regime, or from terminating transients which occur at the opening of an a.-c. circuit.

*Regular Transients with Apparent Distortion.*—In the case represented by Fig. 9, the e.m.f. and current waves, launched without appreciable splash, develop regular transients that build into the final steady state, without noticeable distortion. The successive alternations increase in size without departing noticeably from their sinusoidal shape. This is for the reason that the successive reflections, so long as they are of appreciable magnitude, happen to make their appearance, at each end of the line, at or near the moments when the voltage and current are passing through zero. This must always happen, according to theory, when the length of the freed line is a quarter wave for the impressed frequency. If, however, the line has a length distinctly different from a quarter wave, or



FIG. 13. Apparent Distortion of Transients due to Interference of Successive Reflections.

simple multiple thereof; or if the voltage and current waves are recorded at some intermediate point of a freed quarter-wave line, each of the successive reflections will come in during the active part of an alternation. In particular cases, they may happen to arrive

at the crests of successive alternations. In such instances, the waves will change abruptly from one sinusoid to another of different amplitude. The resulting waves may therefore appear to be distorted, or nonsinusoidal, until they are analyzed. An example of this kind is presented in Fig. 13 (Film No. 101). Here the full-length artificial line (1255 km.) is freed at the distant end, and the recording oscillographs of e.m.f. and current are connected to the line at the half-way point (627.5 km. from each end). It will be seen that the impressed e.m.f.  $e_s$  is applied near an instant of zero voltage, and without perceptible splash. The voltage wave  $e_{390}$  at the midlength point, commencing about 2 milliseconds later, rises also without splash, along an approximately sinusoidal curve. Just about the crest of this wave, the first reflection (positive) has had time to return from the distant free end. This reflected wave adds itself to the first arriving wave at the midway point, and so apparently distorts the wave form. These distortions can be noticed for several alternations in  $e_{390}$ , and are due almost wholly, if not entirely, to the superposition of new reflections. The same considerations apply to the current  $i_{390}$  in the line, at the midway point. The electrical connections are indicated in Fig. 14. The first reflected wave of

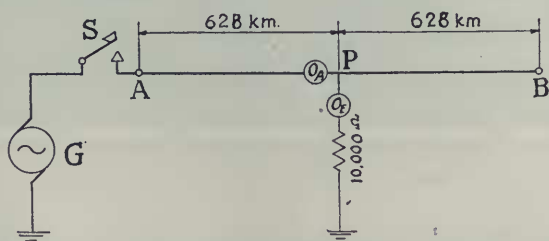


FIG. 14. Electrical Connections of Oscillograph and its Leak, half-way along the Artificial Line freed at B.

current arriving at  $P$ , 4.3 milliseconds after the first arrival at  $P$ , is in the negative direction from the distant free end  $B$ , and so produces a more marked apparent distortion in  $i_{390}$ , than occurs in  $e_{390}$ , where the first reflection is positive. Similar distortions due to further incoming reflections are noticeable in the curve  $i_{390}$  for several alternations. At the end of the oscillogram, 125 milliseconds from the start, the waves of  $e_{390}$  and  $i_{390}$  have very nearly attained their final steady and practically sinusoidal values.

*Analysis of Regular Transient Case.*—Fig. 15 presents the theoretical stationary vector analysis of the case to which the oscillo-

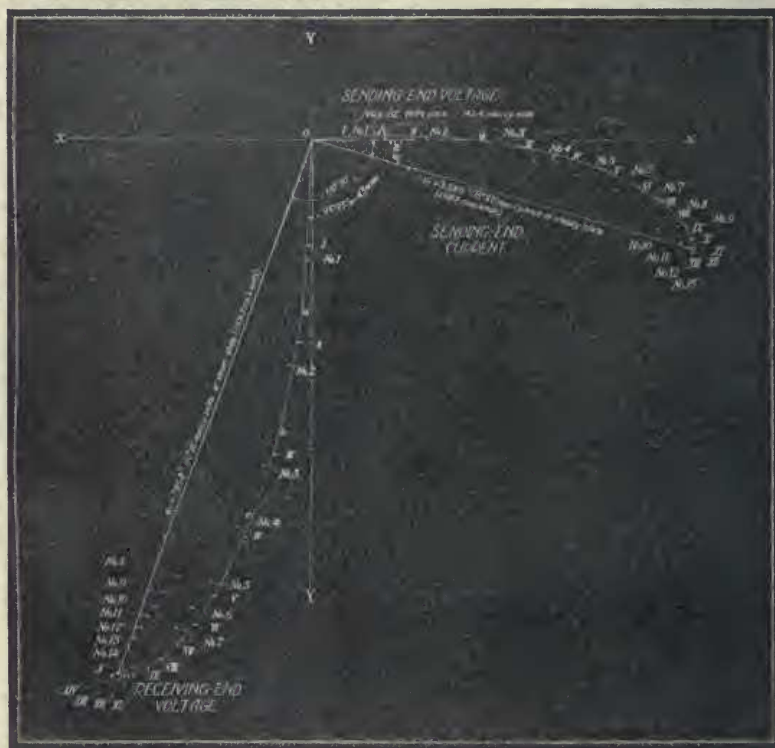


FIG. 15. Vector Diagram of Electromagnetic Terminal Reflections in Long Distance Power Transmission Line.

gram of Fig. 9 belongs. It is treated in detail in Appendix II. The axis  $OX$  represents the standard phase of the sending end voltage. The successive maximum cyclic voltage reflections at  $B$ , are represented to scale by the vectors  $Oa, ab, bc$ , etc., as far as the fourteenth inclusive. The vector sum of these ( $Oa, Ob, Oc$ , etc.) are given for each step in the process. Table V. in Appendix II., shows the maximum cyclic values attained at each stage. This increases to  $E_B 796.2 \sphericalangle 109^\circ.49'$  at the thirteenth reflection. After this, it diminishes slightly to  $795.8 \sphericalangle 110^\circ.36'$  in the final steady state. The final voltage at  $B$  is thus 5.63 times the impressed volt-

age at  $A$ , owing to the fact that the line  $AB$  is nearly of quarter-wave length.<sup>9</sup>

In a similar manner, the successive currents and reflections at  $A$  are indicated by the vectors  $OA$ ,  $AB$ ,  $BC$ , etc., together with the successive vector sums  $OA$ ,  $OB$ ,  $OC$ , etc., as far as the thirteenth wave inclusive, when the final steady state is nearly reached.

We should therefore expect that the voltage at  $B$  would, in the first wave, attain the crest value  $Oa$ , in the next reflection the crest value  $Ob$ , in the next following reflection  $Oc$ , and so on. A comparison between the observed and computed waves is given graphically in Fig. 16. Here the upper line of waves deals with the sending-end current, the middle series with the impressed voltage, and the lowest series with the voltage at  $B$ . Referring to the latter series, the successive reflected voltage waves  $Oa$ ,  $ab$ ,  $bc$ , etc., of Fig. 15, are marked with the numerals I., II., III., etc., in Fig. 16, and these are superposed, by point to point addition, in the heavy wavy line No. 1, No. 2, No. 3, etc. This heavy wave is the computed resultant regular transient of  $e_r$ . If there were no errors in the assumptions or mode of computation, the oscillogram of  $e_r$  should coincide with this line. The oscillogram of  $e_r$  in Fig. 9 actually does coincide very nearly with this theoretical line, the small derivations therefrom being indicated at the crests of the first few waves. Thus, at the crest of wave No. 3, the computed maximum value is 531.9 volts; whereas the oscillograph shows 539 volts, a deviation of 1.3 per cent. This is the largest discrepancy detected between the observed and computed values of  $e_r$ . We are, therefore, entitled to conclude that in the case of this artificial line, with the switch closed splashlessly, the lumpiness of the line had very little effect upon the voltage at the distant free end.

Referring to the upper line of waves  $i_s$  in Fig. 16, the same procedure has been followed. The heavy line is the sum of the reflected waves, according to the vector sums  $OA$ ,  $OB$ ,  $OC$ , of Fig. 15. This heavy wavy line is, therefore, the theoretical summation

<sup>9</sup> If the line had been freed at  $B$ , instead of being grounded through the oscillograph of 9900 ohms, the final voltage  $E$  at  $B$  would have been increased from  $E \times 5.63 \angle 110^\circ 36'$  to  $E \times 6.82 \angle 116^\circ 20'$ , and the transient e.m.f. waves would also have been materially modified.

TRAVELING ELECTROMAGNETIC WAVES AND TERMINAL REFLECTIONS  
 IN LONG DISTANCE POWER TRANSMISSION LINE.



FIG. 16.

of regular current transients at  $A$ . The oscillogram of  $i_s$  should coincide with this line, if there were no errors in assumptions or computation. The actual oscillographed  $i_s$  wave is shown by a chain line in Fig. 16, and the deviations of this from the heavy line are marked thereon at the successive crests. It will be seen that, in the first wave, the discrepancy is small. The discrepancy increases up to wave No. 3, when it reaches 17.5 per cent. The discrepancy then dies away, almost to zero, in the last wave, No. 13.

This discrepancy in current amplitude, reaching a maximum at the third wave, is too large to be attributable to errors of interpretation in the oscillogram. It may be attributed therefore either to

- (1) small higher harmonics in the wave of impressed e.m.f.; *i.e.*, to deviation from the sinusoidal form, with initial wave transients resulting therefrom,
- (2) imperfect regulation of impressed e.m.f., or initial deviation of  $e_s$  from the normal amplitude, with initiating wave transients resulting therefrom,
- (3) lumpiness in the artificial line, with corresponding initiating wave transients,
- (4) secondary reflections at  $A$  from the internal impedance of the alternator, not taken into account.

The shares of the above possible sources of discrepancy in  $i_s$  have not been determined. It is intended, however, to substitute a tapering pair of smaller  $\pi$  sections, for the first section at the  $A$  end of the line, so as to diminish the lumpiness of the line at the generating end, where the waves start. Ordinarily, the greatest discrepancies between theory and observation are to be expected in the initiating wave transients of current at the sending end. All errors are exaggerated at this point. Considering the complexity of the conditions, it is remarkable that the discrepancies have not been larger.

Of the considerable number of initiating wave transient oscillograms which have been obtained on this and other artificial lines, Fig. 9 is a fair sample, and not a specially selected case. It has been analyzed to a greater extent, however, than any of the rest. The conclusion to be drawn from this analysis seems to be sup-

ported by other cases, so far as they have been examined; namely, that at the impressed frequency of  $60\sim$ , nearly sinusoidal, if the voltage is impressed without splash at an instant of zero e.m.f., the artificial line behaves substantially like its conjugate smooth line, the greatest discrepancy being in the current-wave transient at the sending end. Consequently, any similar artificial line of a like degree of lumpiness, should be available, in the laboratory, for the study of initiating and casual a.-c. wave transients.

*Arrival Times.*—The apparent velocity of transmission of an a.-c. wave over an artificial line subtending an angle of  $\theta = \theta_1 + j\theta_2$  hyps radians  $\angle$ , at a given impressed frequency  $f \sim$  is<sup>10</sup>

$$v = \frac{L\omega}{\theta_2} \quad \frac{\text{km.}}{\text{sec.}}, \quad (4)$$

where  $L$  is the length of the line in kilometers. This velocity is the "group velocity" of the waves at this frequency. For the artificial line considered, at  $60.6\sim$ ,  $v = 292,300$  km./sec. It tends to reach the limit 300,000 km./sec. at very high frequencies, in air.

The number of single passages, or single transits, of the wave over the line per second, is

$$n = \frac{v}{L} = \frac{\omega}{\theta_2} \quad \frac{\text{numeric}}{\text{sec.}}. \quad (5)$$

In the case of this line at  $60.6\sim$ ,  $n = 232.9$  transits per second. The transit time  $T$ , or time interval of a single passage over the line, from one end to the other, is\*

$$T = \frac{1}{n} = \frac{\theta_2}{\omega} \quad \text{seconds.} \quad (6)$$

In the case to which Fig. 9 refers,  $\theta_2 = 1.041$  quadrants, and  $\omega = 60.6 \times 4 = 242.4$  quadrants per second. Hence,  $T = 0.004295$  second, or nearly 4.3 milliseconds. At a point  $P$ , whose angular distance from the ends  $A$  and  $B$  are  $\theta' = \theta_1' + j\theta_2'$  and  $\theta'' = \theta_1''$

<sup>10</sup> Bibliography 30, p. 283.

\* Bibliography 30, p. 283.



+  $j\theta_2''$  hyps respectively, the *arrival time*, or time of transit from  $A$  to  $P$  is

$$T_1 = \frac{\theta_2'}{\omega} \quad \text{seconds.} \quad (7)$$

The time required for the wave to go from  $A$  past  $P$  to  $B$ , and back to  $P$ , thus making one reflection from the distant end, will be

$$T_{P1} = \frac{\theta_2' + 2\theta_2''}{\omega} = \frac{2\theta_2 - \theta_2'}{\omega} = 2T - T_1 \quad \text{seconds.} \quad (8)$$

This interval may be called the *B reflection time* at the point  $P$ .

The second *B* reflection at  $P$  arrives after a time  $T_{P2}$  from switch closure

$$T_{P2} = 2T + T_{P1} = \frac{4\theta_2 - \theta_2'}{\omega} = 4T - T_1 \quad \text{seconds.} \quad (9)$$

Similarly, the  $k$ th arrival at  $P$  occurs after a time from switch closure of

$$2(k-1)T + T_1 = \frac{2(k-1)\theta_2 + \theta_2'}{\omega} \quad \text{seconds.} \quad (10)$$

Again, the  $k$ th reflection from the *B* end reaches  $P$  after a time  $T_{Pk}$  from switch closure,

$$T_{Pk} = 2(k-1)T + T_{P1} = \frac{2k\theta_2 - \theta_2'}{\omega} = 2kT - T_1 \quad \text{seconds.} \quad (11)$$

In the case when  $P$  is situated at  $B$ , as in the example of Fig. 9,  $\theta' = \theta$ ,  $\theta'' = 0$ , so that

$$T_{B1} = \frac{\theta_2}{\omega} = T \quad \text{seconds.} \quad (12)$$

and

$$T_{Bk} = 2(k-1)T + T = (2k-1)T \quad \text{seconds.} \quad (13)$$

*Instantaneous Value of Growth Factor.*—If a sinusoidal e.m.f. of  $E_A$  max. cyclic volts, at standard phase, is impressed on the  $A$  end of the line at an instant of zero voltage, then the instantaneous

value at  $A$ ,  $t$  seconds after switch closing, will be

$$e_A = E_A \sin \omega t \quad \text{volts. (14)}$$

As shown in Appendix I., the vector voltage at  $P$  in the final steady state will be<sup>11</sup>

$$E_{P\alpha} = E_A \frac{\sinh \delta_P}{\sinh \delta_A} \quad \text{max. cy. volts. } \angle. \quad (15)$$

The size of  $E_{P\alpha}$  is the size of this planevector quantity, and may be represented by  $|E_{P\alpha}|$ . If its slope is  $-\beta^\circ$ , then the instantaneous value at  $P$  in the steady state, after  $t$  seconds, is

$$P_{P\alpha} = |E_{P\alpha}| \sin(\omega t - \beta^0) \quad \text{inst. volts. (16)}$$

It is also shown in Appendix I. that at  $P$ , after the passage of the  $k$ th reflection from  $B$ , and before the arrival of the  $(k+1)$ th reflection from  $A$ , the max. cyclic vector voltage is

$$E_{Pk} = E_{P\alpha} (1 - \epsilon^{-2k\delta_A}) = E_{P\alpha} \cdot 2\epsilon^{-k\delta_A} \sinh k\delta_A \quad \text{max. cy. volts. } \angle. \quad (17)$$

If the size of this planevector quantity be denoted by  $|E_{Pk}|$ , and its slope is  $-\beta_k^\circ$ ; then at any time  $t$  between the  $k$ th and  $(k+1)$ th reflections, the instantaneous e.m.f. at  $P$  will be

$$e_{Pk} = |E_{Pk}| \sin(\omega t - \beta_k^0) \quad \text{inst. volts. (18)}$$

The slope  $-\beta_k^\circ$  changes abruptly at each succeeding increment.

*Graphical Development of Initiating Transients.*—A rotatory vector diagram of the voltage developed at the  $B$  end of the line in the case represented by Fig. 3, is indicated in Fig. 17, for the first four reflections. The line  $-XOX$  is the projection axis. Projections on this axis from a rotating vector e.m.f. indicate the instantaneous e.m.f. at the end  $B$  of the line, with the oscillograph load of 9900 ohms.

The vector  $OA$  represents the first reflected wave of 239.5 max. cy. volts at  $B$ , at the instant of its arrival there, and when its instantaneous value is still zero. This vector  $OA$  then rotates

<sup>11</sup> Bibliography 30.



size equal to that of  $OB$ , as obtained by consulting the stationary vector diagram Fig. 15.  $OB$  is now the new rotating vector, but its projection on  $OX$  must commence at the same value  $Ob$  as existed at the instant of the second reflection's arrival. This requires an instantaneous leap of the projecting vector from  $OB'$  to  $OB$ . The new vector  $OB$  now executes the half circle  $BC'$  ( $187^\circ$ ) at the standard angular velocity, until it reaches the position  $OC'$ , 8.6 milliseconds later than that it occupied at  $OB$ . Here the third reflection arrives and requires an instantaneous change of the vector from  $OC'$  to  $OC$ , with a common instantaneous projection  $Oc$ . The new resultant vector  $OC$ , of three reflections, now rotates through  $187^\circ$  to  $OD'$ , when the fourth reflection arrives and causes an immediate change to  $OD$ . This process goes on indefinitely. It will be observed that although Fig. 17 represents the instantaneous e.m.f. at the receiving end of the line from the moment of arrival of the first reflection, the angular position of the rotating vector ceases to correspond to the time which has elapsed, owing to the instantaneous backward leaps at the moments when new reflections arrive.

It may be observed that, referring to Fig. 15, the envelope of the successive resultants of e.m.f. reflections  $Oa, b, c$ , etc., is an equiangular spiral. The same is true for the corresponding envelope of current-wave reflections, as laid down in a stationary vector diagram  $O A B C$ , etc., Fig. 15. When the successive waves of arrival and reflection are summed at a point  $P$  along the line, instead of at the distant end  $B$ , the same propositions will be found to apply to the envelope of the successive reflections. The vectors of arriving waves will, however, differ, in general, from those of the reflections succeeding them.

The algebraic expression corresponding to Fig. 17 is:

$$e_B = E_{Am} \{ m\epsilon^{-\theta_1} \sin(\omega t - \theta_2) + m(1 - m)\epsilon^{-3\theta_1} \sin(\omega t - 3\theta_2) \\ + m(1 - m)^2 \epsilon^{-5\theta_1} \sin(\omega t - 5\theta_2) + \dots \} \text{ inst. volts. (18a)}$$

Here each term must be included after the time has elapsed for its arrival. Three phase angles present themselves in each term;

namely, (1) the phase angle  $\omega t$ , which increases uniformly with  $t$ , the time elapsed from switch closure; (2) the angle  $\theta_2, 3\theta_2, 5\theta_2$ , etc., which is a multiple of the circular angle  $\theta_2$  subtended by the line, and is the phase delay due to 1, 3, 5, etc., wave passages over the line; (3) the slope of the vector coefficient  $m, m(1 - m)$ , etc., which takes into account the change of phase in the voltage wave due to reflections. The scalar sum of the terms in (18a) agrees at any instant with the projection on  $OX$  in Fig. 17.

#### SUMMARY.

1. Oscillographic measurements over a lumpy artificial power-transmission line in the laboratory, are reported for certain initiating wave transients. The technique is described. One of these oscillographs is analyzed, and compared with the elementary theory of steady-state attainment. The discrepancies between the observed and computed values are negligible for the voltage waves at the receiving end of the line. They are distinct, but not very serious, for the outgoing current waves at the sending end.

2. A lumpy artificial line can be used for the measurement of initiating a.-c. wave transients, if an automatic circuit-closing switch is set to connect the generator to the line at a moment of zero e.m.f.

3. A provisional classification of transients is offered. Particular cases of splash transients, lumpiness transients, casual transients, and regular initiating transients are offered, from experimental observations.

4. The growth factor of a regular series of transients is analyzed for any point  $P$  in a single line loaded at the receiving end. This growth is a discontinuous function of time, its increase occurring by little vector jumps. The envelope of the growth-factor vector is an equiangular spiral. The growth factors for current and voltage are the same.

5. The transitory impedance at and beyond any one point on a line such as is described, is constant at successive  $B$  reflections, after the first reflection from  $B$ , and is equal to the impedance at that point in the final steady state.

6. The position angle of the  $B$  end of a loaded line in the steady

state is directly related to the transient transmission and reflection coefficients, at that end, during the preliminary state.

7. The process of transmitting power along an alternating-current line may be simply conceived of as the rate of delivery, at the sending end, of magnetic and electric fluxes, with their necessarily contained energies.

#### APPENDIX I.

##### *On the Regular Attenuation of Sinusoidal Waves over a Smooth Uniform Line Loaded with an Impedance at the Receiving End.*

In Fig. 3, let the smooth uniform line  $AB$  be voltaged at  $A$  and loaded at  $B$  with an impedance  $\sigma$  vector ohms (or ohms  $\angle$ ). The switch is closed at  $A$  without splash, on a single-frequency alternator of negligible internal impedance and frequency  $f \sim$ , generating 1 volt maximum cyclic e.m.f. The line has a total conductor impedance  $Z = R + jL\omega$  ohms  $\angle$ , and a total dielectric admittance of  $Y = G + jC\omega$  mhos  $\angle$ , where

- $R$  = total conductor resistance (ohms),
- $L$  = total conductor inductance (henrys),
- $G$  = total dielectric conductance (mhos),
- $C$  = total dielectric capacitance (farads),
- $\omega = 2\pi f$  (radians per sec.).

Required the development with time of voltage and current at the arbitrary point  $P$ , distant  $\theta'$  hyps  $\angle$  from  $A$ , and  $\theta''$  hyps  $\angle$  from  $B$ , the total angle subtended by the line  $AB$  being

$$\theta = \theta' + \theta'' = \sqrt{ZY} = \theta_1 + j\theta_2 \quad \text{hyps } \angle. \quad (19)$$

The surge impedance of the line is

$$z_0 = \sqrt{\frac{Z}{Y}} \quad (\text{ohms } \angle). \quad (20)$$

*E.m.f. Waves or Electrostatic Flux Waves.*—The initial outgoing wave of e.m.f. at  $A$ , when  $t=0$ , is represented by a vector

of 1.0  $\angle$  0° volt max. cyclic value. After this wave of e.m.f. has reached  $P$ , it will have attenuated to the vector perunitage

$$\epsilon^{-\theta'} = \epsilon^{-(\theta_1' + j\theta_2')} = \epsilon^{-\theta_1'} \times \epsilon^{-j\theta_2'} = \epsilon^{-\theta_1'} \sphericalangle \theta_2' \quad \text{numeric } \angle. \quad (21)$$

where  $\theta_2'$  is expressed in real circular radians (or imaginary hyperbolic radians), lagging in phase behind the generator e.m.f. at that moment. When the wave has reached  $B$ , the receiving end of the line, its condition will be  $e^{-\theta} = e^{-\theta_1} \sphericalangle \theta_2$ . At the junction  $BC$ , the wave breaks into a transmitted and reflected component. If the transmission coefficient is  $m$ , then, following in planevector notation what Heaviside<sup>12</sup> first showed, with real numbers only, for the distortionless case:

$$m = \frac{\frac{\sigma}{z_0 + \sigma}}{2} = \frac{2\sigma}{z_0 + \sigma} \quad \text{numeric } \angle, \quad (22)$$

and the e.m.f. transmitted to  $\sigma$  at  $C$  is  $me^{-\theta}$  volts  $\angle$ . (23)

The voltage for reflection at  $B$  will be  $(1 - m)e^{-\theta}$  volts. This voltage is directed back from  $B$  towards  $A$ , and should be counted as  $-(1 - m)e^{-\theta} = (m - 1)e^{-\theta}$  volts  $\angle$  on the line.

The time required for the wave to reach  $P$  from  $A$  will be  $\theta_2'/\omega$  seconds, and to reach  $B$ ,  $\theta_2/\omega$  seconds. This is the traverse time of the line and may be denoted by  $T$ . We may therefore represent the progress of the wave by the following table. The assumption is made as a first approximation, that the generator at  $A$  has negligible internal impedance; *i.e.*, that the effect of its internal e.m.f., acting in conjunction with reflections from its actual internal impedance, is the same as its terminal e.m.f. steadily impressed at  $A$  would have with zero internal impedance (Table III.). Here  $\delta_B$  is the position angle at the end  $B$  of the line in the steady state or  $\tanh^{-1}(\sigma/z_0)$ . Again  $\delta_A = \theta + \delta_B$  is the position angle at the end  $A$  of the line in the steady state. Also  $\delta_P = \theta'' + \delta_B = \delta_A - \theta'$  is the position angle at the selected point  $P$  of the line in the steady state. It is well known that, in the steady state, if the impressed voltage at  $A$  is 1.0  $\angle$  0° max. cy. volts, the final voltage at  $P$  is  $(\sinh \delta_P)/(\sinh \delta_A)$ .

<sup>12</sup> Bibliography 1.

TABLE III.

SCHEDULE OF VOLTAGE WAVE ARRIVALS AND REFLECTIONS AT A POINT  $P$  ON A UNIFORM LINE  $AB$ , ON WHICH UNIT MAX. CY. E.M.F. IS IMPRESSED AT  $A$ , AND A LOAD  $\sigma$  VECTOR OHMS IS CONNECTED AT  $B$ .

| No. of Wave, | Time at $A$ ,<br>$t$ Secs. | $A$ .   | $P$ .   | $B$ .   | $C$ .   | Time at $C$ ,<br>$t$ Secs. |
|--------------|----------------------------|---|---|---|---|----------------------------|
| 1A           | 0                          | 1.0   | $\epsilon^{-\theta'}$   | $\epsilon^{-\theta}$  | $m\epsilon^{-\theta}$   | $T$                        |
| 1R           | $2T$                       | $(m-1)\epsilon^{-2\theta}$  | $(m-1)\epsilon^{-(2\theta-\theta')}$  | $(m-1)\epsilon^{-\theta}$   |   | $T$                        |
| 2A           | $2T$                       | $(1-m)\epsilon^{-2\theta}$  | $(1-m)\epsilon^{-(2\theta+\theta')}$  | $(1-m)\epsilon^{-3\theta}$  | $m(1-m)\epsilon^{-3\theta}$   | $3T$                       |
| 2R           | $4T$                       | $-(m-1)^2\epsilon^{-4\theta}$   | $-(m-1)^2\epsilon^{-(4\theta-\theta')}$   | $-(m-1)^2\epsilon^{-3\theta}$   |   | $3T$                       |
| 3A           | $4T$                       | $(1-m)^2\epsilon^{-4\theta}$  | $(1-m)^2\epsilon^{-(4\theta+\theta')}$  | $(1-m)^2\epsilon^{-5\theta}$  | $m(1-m)^2\epsilon^{-5\theta}$   | $5T$                       |
| 3R           | $6T$                       | $(m-1)^3\epsilon^{-6\theta}$  | $(m-1)^3\epsilon^{-(6\theta-\theta')}$  | $(m-1)^3\epsilon^{-5\theta}$  |   | $5T$                       |
| ...          | ...                        | ...   | ...   | ...   | ...   | ...                        |
| kA           | $2(k-1)T$                  | $(1-m)^{k-1}\epsilon^{-2\theta(k-1)}$<br>$= \epsilon^{-2(k-1)\delta_A}$ | $(1-m)^{k-1}\epsilon^{-\{2(k-1)\theta+\theta'\}}$<br>$= \epsilon^{-2(k-1)\delta_A+\theta'}$ | $(1-m)^{k-1}\epsilon^{-(2k-1)\theta}$<br>$= \epsilon^{-(2k-1)\delta_A+\delta_B}$  | $m(1-m)^{k-1}\epsilon^{-(2k-1)\theta}$<br>$= 2 \sinh \delta_B \epsilon^{-(2k-1)\delta_A}$ | $(2k-1)T$                  |
| kR           | $2kT$                      | $-(1-m)^k\epsilon^{-2k\theta}$<br>$= -\epsilon^{-2k\delta_A}$           | $-(1-m)^k\epsilon^{-(2k\theta-\theta')}$<br>$= -\epsilon^{(2k\delta_A-\theta')}$            | $-(1-m)^k\epsilon^{-(2k-1)\theta}$<br>$= -\epsilon^{-(2k-1)\delta_A-\delta_B}$    |   | "                          |
| Sum to       | $2kT$                      | 1.0   | $\sinh \delta_P (1 - \epsilon^{-2k\delta_A})$<br>$\sinh \delta_A$                           | $\sinh \delta_B (1 - \epsilon^{-2k\delta_A})$<br>$\sinh \delta_A$                 |   | Sum to<br>$2(k-1)T$        |
| "            | "                          | 1.0   | $\sinh \delta_P \cdot 2\epsilon^{-k\delta_A} \sinh k\delta_A$<br>$\sinh \delta_A$           | $\sinh \delta_B \cdot 2\epsilon^{-k\delta_A} \sinh k\delta_A$<br>$\sinh \delta_A$ |   | "                          |
| "            | "                          | 1.0   | $E_{P\infty} \cdot 2\epsilon^{-k\delta_A} \sinh k\delta_A$                                  | $E_{B\infty} \cdot 2\epsilon^{-k\delta_A} \sinh k\delta_A$                        |   | "                          |



Consequently, if instead of taking the final voltage at  $P$  in the steady state, we take the stage of voltage growth at  $P$  found after  $k$  reflections from  $B$  have passed  $P$ , the corresponding vector stage of  $E_P$ , which may be denoted by  $E_{Pk}$ , is

$$E_{Pk} = E_{P\infty}(1 - \epsilon^{-2k\delta_A}) = E_{P\infty}(2\epsilon^{-k\delta_A} \sinh k\delta_A) \quad \text{volts } \angle. \quad (24)$$

The vector coefficient within the brackets may be described as the vector coefficient of growth,  $k$  being an integer, increasing by unit steps. At  $k = \infty$ , this coefficient reaches unity. It is a real coefficient, or has no imaginary component, when the imaginary part of  $\delta_A$  is a quadrant or any integral number of quadrants. Thus, if the line with its load at  $B$  develops a quarter-wave length at  $A$ ; so that  $\delta_A$  contains one imaginary quadrant, then  $e^{-2k\delta_A}$  is a real number, and so is the coefficient of growth at all stages. The phase of the final voltage at  $P$  will then be the same as that at the arrival of the first wave.

*Current Waves or Magnetic Flux Waves.*—If the e.m.f. impressed on  $A$  is  $1.0 \angle 0^\circ$  max. cy. volts, without splash, the initial outgoing current at  $A$  is  $1 \angle 0^\circ / z_0 = E_A y_0 = I_0$  amperes  $\angle$ , where  $y_0$  is the surge admittance  $1/z_0$ . The first current wave arrival at  $P$  finds this attenuated to  $I_0 e^{-\theta'}$  and the first arrival at  $B$  to  $I_0 e^{-\theta'}$  vector amperes. In each successive arrival, the value  $I_0$  appears, and in tabulating the wave progress,  $I_0$  may be omitted as a common multiplier throughout, until the summation is effected. We may therefore prepare a schedule of reflections similar to that given for the waves of e.m.f. The coefficients of transmission and reflection of the current waves arriving at  $B$  are however different from those for the voltage waves. The coefficient of current-wave transmission  $n$  is

$$n = \frac{z_0}{\left(\frac{z_0 + \sigma}{2}\right)} = \frac{2z}{z_0 + \sigma} \quad \text{numeric } \angle \quad (25)$$

and the reflection coefficient is

$$n - 1 = \frac{z_0 - \sigma}{z_0 + \sigma} \quad \text{numeric } \angle, \quad (26)$$

TABLE IV.

SCHEDULE OF CURRENT WAVE ARRIVALS AND REFLECTIONS AT A POINT  $P$  ON A UNIFORM LINE  $AB$ , ON WHICH A CURRENT OF MAX. CY. STRENGTH  $I_0 = E/Z_0$  VECTOR AMPERES IS LAUNCHED AT  $A$ , AND TO WHICH A LOAD OF  $\sigma$  VECTOR OHMS IS CONNECTED AT  $B$ .

| No. of Wave.       | Time at $A$ , $t$ Secs. | $A$ .  | $P$ .   | $B$ .  | $C$ .   | Time at $C$ , $t$ Secs. |
|--------------------|-------------------------|--|---|--|---|-------------------------|
| $1A$               | $0$                     | $1.0$  | $\epsilon^{-\theta'}$   | $\epsilon^{-\theta}$   | $n\epsilon^{-\theta}$   | $T$                     |
| $2A$               | $2T$                    | $(n-1)\epsilon^{-2\theta}$   | $(n-1)\epsilon^{-(2\theta-\theta')}$  | $(n-1)\epsilon^{-\theta}$  | $n(n-1)\epsilon^{-3\theta}$   | $T$                     |
| $2R$               | $2T$                    | $(n-1)\epsilon^{-2\theta}$   | $(n-1)\epsilon^{-(2\theta+\theta')}$  | $(n-1)\epsilon^{-3\theta}$   | $n(n-1)\epsilon^{-3\theta}$   | $3T$                    |
| $4A$               | $4T$                    | $(n-1)^2\epsilon^{-4\theta}$   | $(n-1)^2\epsilon^{-(4\theta-\theta')}$  | $(n-1)^2\epsilon^{-3\theta}$   | $n(n-1)^2\epsilon^{-5\theta}$   | $3T$                    |
| $3A$               | $4T$                    | $(n-1)^2\epsilon^{-4\theta}$   | $(n-1)^2\epsilon^{-(4\theta+\theta')}$  | $(n-1)^2\epsilon^{-5\theta}$   | $n(n-1)^2\epsilon^{-5\theta}$   | $5T$                    |
| $3R$               | $6T$                    | $(n-1)^3\epsilon^{-6\theta}$   | $(n-1)^3\epsilon^{-(6\theta-\theta')}$  | $(n-1)^3\epsilon^{-5\theta}$   | $n(n-1)^3\epsilon^{-5\theta}$   | $5T$                    |
| ...                | ...                     | ...  | ...   | ...  | ...   | ...                     |
| $kA$               | $2(k-1)T$               | $(n-1)^{k-1}\epsilon^{-2(k-1)\theta}$<br>$= \epsilon^{-2(k-1)\delta_A}$  | $(n-1)^{k-1}\epsilon^{-2(k-1)\theta+\theta'}$<br>$= \epsilon^{-2(k-1)\delta_A+\theta'}$ | $(n-1)^{k-1}\epsilon^{-(2k-1)\theta}$<br>$= \epsilon^{-2(k-1)\delta_A-\theta}$ | $n(n-1)^{k-1}\epsilon^{-(2k-1)\theta}$<br>$= 2 \cosh \delta_B \epsilon^{-(2k-1)\delta_A}$ | $(2k-1)T$               |
| $kR$               | $2kT$                   | $(n-1)^k \epsilon^{-2k\theta} = \epsilon^{-2k\delta_A}$                  | $(n-1)^k \epsilon^{-(2k\theta-\theta')} = \epsilon^{-(2k\delta_A-\theta')}$             | $(n-1)^k \epsilon^{-(2k\delta_A-\theta)}$<br>$= \epsilon^{-2k\delta_A}$        |   | $(2k-1)T$               |
| Sum to             | $2kT$                   | $I_0 \frac{\cosh \delta_A}{\sinh \delta_A} (1 - \epsilon^{-2k\delta_A})$ | $I_0 \frac{\cosh \delta_P}{\sinh \delta_A} (1 - \epsilon^{-2k\delta_A})$                | $I_0 \frac{\cosh \delta_B}{\sinh \delta_A}$                                    | $I_0 \frac{\cosh \delta_B}{\sinh \delta_A} (1 - \epsilon^{-2k\delta_A})$                  | Sum to                  |
| "                  | "                       | $I_A \frac{\cosh \delta_A}{\cosh \delta_A} (1 - \epsilon^{-2k\delta_A})$ | $I_A \frac{\cosh \delta_P}{\cosh \delta_A} (1 - \epsilon^{-2k\delta_A})$                | $I_A \frac{\cosh \delta_B}{\cosh \delta_A}$                                    | $I_A \frac{\cosh \delta_B}{\cosh \delta_A} (1 - \epsilon^{-2k\delta_A})$                  | "                       |
| "                  | "                       | $I_{A\alpha} (1 - \epsilon^{-2k\delta_A})$                               | $I_{P\alpha} (1 - \epsilon^{-2k\delta_A})$  | $I_{B\alpha} (1 - \epsilon^{-2k\delta_A})$                                     | $I_{B\alpha} (1 - \epsilon^{-2k\delta_A})$  | "                       |
| "                  | "                       | $I_{A\alpha} \cdot 2\epsilon^{-2k\delta_A} \sinh k\delta_A$              | $I_{P\alpha} \cdot 2\epsilon^{-k\delta_A} \sinh k\delta_A$                              | $I_{B\alpha} \cdot 2\epsilon^{-k\delta_A} \sinh k\delta_A$                     | $I_{B\alpha} \cdot 2\epsilon^{-k\delta_A} \sinh k\delta_A$                                | "                       |
| including $(k+1)A$ | $2kT$                   | $I_{A\alpha} (1 - \epsilon^{-2k\delta_A}) + I_{0\epsilon^{-2k\delta_A}}$ |   |  |   |                         |

so that in terms of  $m$ ,

$$n = 2 - m \quad \text{numeric } \angle \quad (27)$$

and

$$n - 1 = 1 - m \quad \text{numeric } \angle \quad (28)$$

These rules are of general application, and may be thus expressed. The sum of the voltage and current transmission coefficients at a junction point in a line is equal to 2. The two reflection coefficients have the same size, but have mutually opposite signs.

#### APPENDIX II.

*On the Case of Line AB Connected as in Fig. 1, and Oscillographed as in Fig. 9 (Film No. 40), with 100 Volts R.m.s. Sinusoidal, Impressed at A, with Negligible Splash and Negligible Lumpiness Transient.*

Taking the tabulated constants of the artificial line from Table II., the impedance of the oscillograph load at B was  $\sigma = 9900 \angle 0^\circ$  ohms. The angle  $\delta_B$  subtended by this load

$$= \tanh^{-1} \frac{9900 \angle 0^\circ}{342.5 \angle 4^\circ 24'} = 0.03451 + j0.9983 \text{ hyp.}$$

This is the position angle  $\delta_B$  of the end B of the line in the steady state. The position angle of the A end is  $\delta_A = \theta + \delta_B = 0.1660 + j2.0393$  hyps.

The e.m.f. at B in the final steady state with  $141.4 \angle 0^\circ$  max. cyclic volts at A will be

$$E_B = 141.4 \angle 0^\circ \times \frac{\sinh(0.03451 + j0.9983)}{\sinh(0.1660 + j2.0393)} = 795.8 \angle 110^\circ 36' \text{ volts.}$$

Similarly, the sending-end final current at A in the steady state is

$$I_s = \frac{E_A}{z_0 \tanh \delta_A} = \frac{141.4 \angle 0^\circ}{342.5 \angle 4^\circ 24' \times 0.17571 \angle 20^\circ 0' 45''}$$

$$= \frac{141.4 \angle 0^\circ}{60.180 \angle 15^\circ 36' 45''} = 2.350 \angle 15^\circ 36' 45'' \text{ amperes.}$$

Comparing these values with those taken from the oscillograph Fig. 9,  $E_r = 796 \nabla 110^\circ$  max. cyclic volts, and  $I_s = 2.35 \nabla 15^\circ$  max. cy. amperes. This agreement is satisfactory, and is even closer than the interpretation of the oscillograph record would warrant. The width of the curves in Fig. 9 is greater than in subsequent oscillographs, when the optical technique had been improved; so that the precision of measurement in Fig. 9 is somewhat below that later attained.

It is shown in Appendix I, that with a given load of  $\sigma$  vector ohms, applied at  $B$  to a single smooth line, with a sinewave of unit maximum e.m.f. applied splashlessly at  $A$ , the voltage wave at a point  $P$  on the  $k$ th reflection from the  $B$  end, is

$$- (1 - m)^k \epsilon^{-(2k\theta - \theta')} \text{ max. cy. volts } \angle, \quad (29)$$

where  $m$  is the transmission coefficient to a voltage wave arriving at  $B$ ,  $\theta$  is the angle subtended by the line, and  $\theta'$  the angle from  $A$  to the selected point  $P$ . This expresses both the size and slope of the  $k$ th return wave at  $P$ , with respect to unity size and zero slope, or standard voltage phase, at  $A$ .

The summation of all the e.m.f. waves arriving at the point  $P$ , including the  $k$ th reflected wave from  $B$ , is also shown to be

$$\frac{\sinh \delta_P}{\sinh \delta_A} (1 - \epsilon^{-2k\delta_A}) = \frac{\sinh \delta_P}{\sinh \delta_A} \cdot 2\epsilon^{-k\delta_A} \sinh k\delta_A \text{ max. cy. volts } \angle. \quad (30)$$

But the final steady voltage at  $P$  is  $(\sinh \delta_P)/(\sinh \delta_A)$  volts  $\angle$ ; so that the summation to the  $k$ th return wave at  $P$ , inclusive, is equal to the final voltage multiplied by the vector "growth coefficient"

$$w = 1 - \epsilon^{-2k\delta_A} = 2\epsilon^{-k\delta_A} \sinh k\delta_A \text{ numeric } \angle. \quad (31)$$

If, then, we denote the final max. cyclic voltage at  $P$  by  $E_{P\infty}$  vector volts, the corresponding maximum cyclic voltage at an intermediate period, after the arrival of the  $k$ th return wave from  $B$ , and before the arrival of the next following incoming wave from  $A$ , is

$$E_{Pk} = E_{P\infty} \cdot w \text{ max. cy. volts } \angle. \quad (32)$$

The growth coefficient  $w$  is not a continuous function of time. It increases by a sudden jump at each moment when a new reflected wave arrives. The size of  $w$  is zero up to the time when  $k=1$ , and attains unity when  $k=\infty$ , but it may exceed unity during the process of increase. That is, the max. cyclic voltage  $E_{Pk}$  may happen to be greater at some stage of the regular transient state, than in the final steady state. The slope of  $w$  may also vary over a considerable range during the period of regular transient growth.

Similarly, referring to Appendix I., Table IV. shows that the attenuation coefficient of the current wave at a point  $P$  on the  $k$ th reflection from the  $B$  end of the line is

$$(n - 1)^k \epsilon^{-(2k\theta - \theta')} = \epsilon^{-(2k\delta_A - \theta')} \quad \text{numeric } \angle, \quad (33)$$

where  $n$  is the transmission coefficient of a current wave arriving at  $B$ . The summation of all the current waves arriving at the point  $P$ , including the  $k$ th reflected wave from  $B$ , is also shown to be

$$\begin{aligned} I_{Pk} &= I_A \frac{\cosh \delta_P}{\cosh \delta_A} (1 - \epsilon^{-2k\delta_A}) \\ &= I_A \frac{\cosh \delta_P}{\cosh \delta_A} \cdot 2\epsilon^{-k\delta_A} \sinh k\delta_A \quad \text{max. cy. amperes } \angle, \quad (34) \end{aligned}$$

where  $I_A$  is the max. cy. current at  $A$  in the steady state, ordinarily taken to  $E_A$  as standard phase.

But the max. cyclic current at  $P$  in the steady state is known to be

$$I_{P\infty} = I_A \cdot \frac{\cosh \delta_P}{\cosh \delta_A} = \frac{E_A}{z_0} \cdot \frac{\cosh \delta_P}{\sinh \delta_A} \quad \text{max. cy. amperes } \angle, \quad (35)$$

so that

$$\begin{aligned} I_{Pk} &= I_{P\infty} (1 - \epsilon^{-2k\delta_A}) = I_{P\infty} \cdot 2\epsilon^{-k\delta_A} \sinh k\delta_A \\ &= I_{P\infty} w \quad \text{max. cy. amperes } \angle. \quad (36) \end{aligned}$$

This means that the growth coefficient  $w_k$ , after the passage of the  $k$ th reflection back from  $B$ , is the same for both the voltage and current at  $P$ . It also means that the impedance of the line  $PB$  and

TABLE V.  
THE GROWTH FACTOR.

| $k$      | Growth Factor $w$ ,<br>Numeric $\angle$ . | Receiving-end Voltage Max. cy.<br>Volts $\angle$ . |                             | Sending-end Current, Max. cy. Amps. $\angle$ . |  |                            | Total Vector Resultant,<br>$\angle Ak$ . |
|----------|---|--|-----------------------------|--|--|----------------------------|--|
|          |   | Time M. Sec.                                       | $E, B, k$ .                 | Resultant of $k$ Waves,<br>$\angle A\alpha$ %. | ( $k+1$ )th Reflected<br>Wave, $\angle A(k+1)$ . |                            |  |
| 1        | 0.3012 $\angle$ 17° 3' 32"                | $t$<br>4.3   | 239.7 $\angle$ 93° 32' 28"  | 0.7079 $\angle$ 1° 26' 47"                     | 0.2963 $\angle$ 2° 40' 26"                       | 1.004 $\angle$ 0° 13' 52"  |  |
| 2        | 0.5164 $\angle$ 14° 6' 11"                | 12.9   | 411.0 $\angle$ 96° 29' 49"  | 1.2135 $\angle$ 1° 30' 34"                     | 0.2126 $\angle$ 9° 44' 53"                       | 1.424 $\angle$ 2° 43' 54"  |  |
| 3        | 0.6692 $\angle$ 11° 31' 30"               | 21.5   | 532.5 $\angle$ 90° 4' 30"   | 1.5726 $\angle$ 4° 5' 15"                      | 0.1525 $\angle$ 16° 49' 10"                      | 1.722 $\angle$ 5° 12' 24"  |  |
| 4        | 0.7769 $\angle$ 9° 18' 20"                | 30.1   | 618.3 $\angle$ 101° 17' 40" | 1.8256 $\angle$ 6° 18' 25"                     | 0.1094 $\angle$ 23° 53' 46"                      | 1.930 $\angle$ 7° 17' 19"  |  |
| 5        | 0.8521 $\angle$ 7° 25' 18"                | 38.7   | 678.1 $\angle$ 103° 10' 42" | 2.0024 $\angle$ 8° 11' 27"                     | 0.0785 $\angle$ 30° 58' 12"                      | 2.078 $\angle$ 9° 34' 53"  |  |
| 6        | 0.9040 $\angle$ 5° 50' 43"                | 47.3   | 719.5 $\angle$ 104° 45' 17" | 2.1245 $\angle$ 9° 46' 2"                      | 0.0563 $\angle$ 38° 2' 38"                       | 2.174 $\angle$ 10° 28' 14" |  |
| 7        | 0.9394 $\angle$ 4° 32' 48"                | 55.9   | 747.6 $\angle$ 106° 3' 12"  | 2.2076 $\angle$ 11° 3' 57"                     | 0.0404 $\angle$ 45° 7' 5"                        | 2.241 $\angle$ 11° 38' 27" |  |
| 8        | 0.9631 $\angle$ 3° 29' 23"                | 64.5   | 766.5 $\angle$ 107° 6' 37"  | 2.2634 $\angle$ 12° 7' 22"                     | 0.0290 $\angle$ 52° 11' 31"                      | 2.291 $\angle$ 13° 8' 5"   |  |
| 9        | 0.9789 $\angle$ 2° 38' 42"                | 73.1   | 778.9 $\angle$ 107° 57' 18" | 2.3000 $\angle$ 12° 58' 3"                     | 0.0208 $\angle$ 64° 15' 58"                      | 2.313 $\angle$ 13° 22' 12" |  |
| 10       | 0.9887 $\angle$ 1° 58' 41"                | 81.7   | 786.8 $\angle$ 108° 37' 19" | 2.3233 $\angle$ 13° 38' 4"                     | 0.0149 $\angle$ 66° 26' 24"                      | 2.333 $\angle$ 13° 55' 35" |  |
| 11       | 0.9948 $\angle$ 1° 27' 36"                | 90.3   | 791.7 $\angle$ 109° 8' 24"  | 2.3465 $\angle$ 14° 32' 57"                    | 0.0077 $\angle$ 80° 29' 17"                      | 2.350 $\angle$ 14° 43' 13" |  |
| 12       | 0.9985 $\angle$ 1° 3' 48"                 | 98.9   | 794.5 $\angle$ 109° 32' 12" | 2.3512 $\angle$ 14° 49' 54"                    | 0.0055 $\angle$ 87° 33' 43"                      | 2.352 $\angle$ 14° 57' 35" |  |
| 13       | 1.0005 $\angle$ 0° 46' 51"                | 107.5  | 796.2 $\angle$ 109° 49' 9"  | —  | —  | —                          |  |
| $\infty$ | 1.0000 $\angle$ 0° 0' 0"                  | $\alpha$   | 795.8 $\angle$ 110° 36' 0"  | 2.3500 $\angle$ 15° 36' 45"                    | 0  | 2.350 $\angle$ 15° 36' 45" |  |

the load  $\sigma$ , as developed at  $P$ , will be the same, after the passage of the  $k$ th reflected wave of voltage and current, as in the final steady state or

$$Z_{Pk} = \frac{E_{Pk}}{I_{Pk}} = z_0 \tanh \delta_P = Z_{P\infty} = \text{constant} \quad \text{ohms } \angle. \quad (37)$$

It is here assumed that the  $k$ th reflection of voltage from  $B$  has passed  $P$ , and also the  $k$ th reflection of current, as the two are, in general, dephased by a definite amount.

It may be noted that when, as in Fig. 9, the current is observed at the  $A$  end of the line, the oscillogram includes, with the  $k$ th reflection from  $B$ , the  $(k+1)$ th outgoing wave from  $A$ . The point  $P$  of observation would have to be shifted to a suitable distance from  $A$ , in order to separate these two impulses. Consequently, when summing up the growth of current at  $A$ , the  $(k+1)$ th outgoing wave must be added to  $I_{Pk}$ . This increment is

$$I'_{Ak} = I_0(n-1)^k \epsilon^{-k\theta} = I_0 \epsilon^{-2k\delta_A} \quad \text{max. cy. amperes } \angle. \quad (38)$$

The accompanying Table V. shows the successive values of the growth coefficient  $w$  for the artificial line under test from  $k=1$  to  $k=13$  inclusive, both for voltage at  $B$  and current at  $A$ .

The vector diagram of Fig. 15, shows the planevector increase of voltage at  $B$  and current at  $A$  for the case represented by the oscillogram, Fig. 9. The voltage  $Oa=239.7 \sphericalangle 93^\circ.33'$  and is the first wave at  $B$ , including immediate reflection there. The angle  $XOa=93^\circ.33'$ , or  $OX$ , represents the standard phase of impressed e.m.f. at  $A$ . If the line had been of exactly a quarter wave-length, this angle  $XOa$  would have been reduced to just one quadrant. This wave  $Oa$  commences to arrive at  $B$ , 4.3 milliseconds ( $93^\circ.55$  electrical degrees on a 60.6  $\sphericalangle$  circuit) after closing the switch at  $A$ . The second wave reflection at  $B$  will commence to develop after the outgoing wave has run three times over the line ( $AB, BA, AB$ ), or a total lapse of 12.9 milliseconds after switch closing. Its vector value in the Table is  $172.0 \sphericalangle 100^\circ.37'$  and it is represented by  $ab$  in Fig. 15.

*Relations between the transmission-reflection coefficients in the transient state and the position angle at B in the subsequent steady state:* Referring to Fig. 3, and to the load of  $\sigma$  vector ohms at B connected to a uniform line of surge impedance  $z_0$ , we know that in the steady a.-c. state, the position angle  $\delta_B$  at B is defined by

$$\tanh \delta_B = \frac{\sigma}{z_0} \quad \text{numeric } \angle. \quad (39)$$

But

$$\tanh \delta_B = \frac{\epsilon^{\delta_B} - \epsilon^{-\delta_B}}{\epsilon^{\delta_B} + \epsilon^{-\delta_B}} = \frac{1 - \epsilon^{-2\delta_B}}{1 + \epsilon^{-2\delta_B}} \quad \text{numeric } \angle. \quad (40)$$

Hence

$$1 - \epsilon^{-2\delta_B} = \frac{2\sigma}{z_0 + \sigma} = m = 2 - n = 1.9333 + j0.00496 \\ = 1.9333 \angle 0^\circ 8' 49'' \quad \text{numeric } \angle, \quad (41)$$

$$-\epsilon^{-2\delta_B} = \frac{\sigma - z_0}{z_0 + \sigma} = m - 1 = 1 - n = 0.9333 + j0.00496 \\ = 0.93331 \angle 0^\circ 18' 16'' \quad \text{numeric } \angle, \quad (42)$$

$$1 + \epsilon^{-2\delta_B} = \frac{2z_0}{z_0 + \sigma} = 2 - m = n = 0.0667 - j0.00496 \\ = 0.06689 \angle 4^\circ 15' 10'' \quad \text{numeric } \angle, \quad (43)$$

$$\epsilon^{-2\delta_B} = \frac{z_0 - \sigma}{z_0 + \sigma} = 1 - m = n - 1 = -0.9333 - j0.00496 \\ = 0.93331 \angle 179^\circ 41' 44'' \quad \text{numeric } \angle, \quad (44)$$

$$\delta_B = \text{logh} \sqrt{\frac{1}{1-m}} = \text{logh} \sqrt{\frac{1}{n-1}} = 0.03451 + j1.56814 \\ = 0.03451 + j0.9983 \quad \text{numeric } \angle, \quad (45)$$

Here  $m$  is the voltage transmission

coefficient at junction BC

$-(1-m) = m-1$  is the voltage reflection

coefficient at junction BC

$n$  is the current transmission

coefficient at junction BC

$-(1-n) = n-1$  is the current reflection

coefficient at junction BC



*The Energy Content of an Outgoing Wave.*—Fig. 18 presents a diagrammatic view of a single pair of outgoing waves from the generator  $A$  on to the uniform line  $AB$ ,  $E$  being the voltage wave

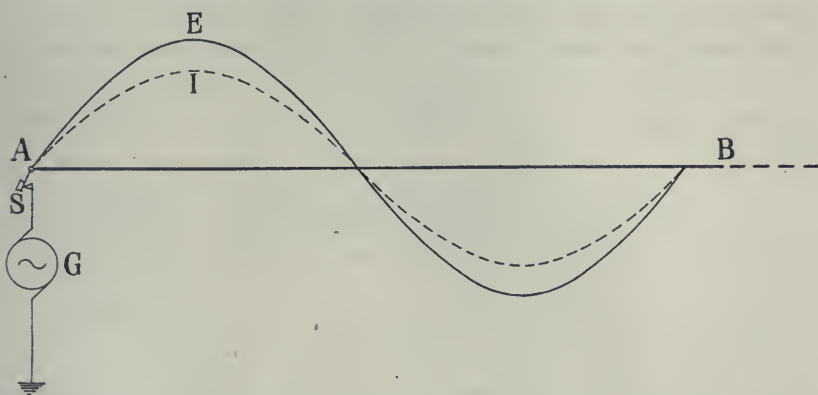


FIG. 18. Diagram of Single Wave Current and E.M.F., launched on a Uniform Distortionless Line.

and  $I$  the current wave. If the line is taken as distortionless, in the simplest case, the two waves will be emitted in cophase. The maximum cyclic value of the sinusoidal impressed e.m.f. being  $E_A$  volts, and the linear capacitance  $c$  farads per km., the electric energy given to the wave in an element of length  $dx$  km. will be  $e^2(c/2)dx$  joules, where  $e$  is the instantaneous value of the e.m.f. The total electric energy in the wave will be  $\frac{E_A^2}{2} \cdot \frac{c}{2} \cdot \lambda$  joules, where  $\lambda$  is the length of the wave in km.; because  $E_A^2/2$  is the average square of  $e$  integrated over the wave-length. This electric energy is distributed in the dielectric in the form  $w_e = B_e^2/8\pi\kappa$  ergs per c.c., where  $B_e$  is the electric flux density in "statgausses," and  $\kappa$  the inductivity of air. The frequency of the impressed e.m.f. being  $f$ , the rate of delivering electric flux energy to the line is

$$P_e = \frac{E_A^2}{2} \cdot \frac{c}{2} \cdot f\lambda = \frac{E_A^2 \cdot c}{4} \cdot v \quad \text{watts.} \quad (46)$$

The wave attenuates as it advances along the line, but the last equation expresses the initial power of supplying electric flux into

the dielectric at the end  $A$  of the line. The quantity  $v$  is the apparent velocity of transmission.

Similarly, if  $l$  is the linear inductance in henrys per km., the sinusoidal outgoing current at  $A$  has an instantaneous value  $i$  and a maximum cyclic value  $I_0$  amperes, the magnetic energy in an element  $dx$  of the line is  $i^2(l/2)dx$  joules. The total magnetic energy in a complete outgoing wave as it passes  $A$  is  $(I_0^2/2) \cdot (l/2) \cdot \lambda$  joules. But

$$I_0 = \frac{E_A}{z_0} = \frac{E_A}{\sqrt{l/c}} = E_A \cdot \sqrt{\frac{c}{l}}; \text{ so that } I_0^2 = E_A^2 \cdot \frac{c}{l},$$

or

$$\frac{I_0^2}{2} \cdot \frac{l}{2} = \frac{E_A^2}{2} \cdot \frac{c}{2} \quad \text{joules. (47)}$$

The magnetic energy in the wave is therefore  $(E^2/2) \cdot (c/2) \cdot \lambda$  joules, which is the same amount as the electric energy. The magnetic energy is distributed in the dielectric as volume energy of magnetic flux of the type  $w_m = B_m^2 / (8\pi\mu)$  ergs per c.c., where  $B_m$  is the magnetic flux density in gausses, and  $\mu$  the permeability of the air.  $B_e = B_m$  numerically, and  $w_e = w_m$  ergs/c.c. The energy of any initial outgoing wave is thus half electric flux energy, and half magnetic energy. The rate of delivering this magnetic energy at  $A$  is

$$P_m = \frac{E_A^2}{2} \cdot \frac{c}{2} \cdot f\lambda = \frac{E_A^2 \cdot c}{4} \cdot v \quad \text{watts. (48)}$$

Thus  $P_m = P_e$ . The total power

$$P = \frac{E_A^2 c}{2} \cdot v = \frac{I_0^2 l}{2} v \quad \text{watts. (49)}$$

The mechanism of electric power transmission, as contemplated in the initial transient state, is the energization of the dielectric with electric and magnetic fluxes, which at each point have equal numerical values and volume energies, and, in shipping off these slabs of flux at the transmission speed  $v$ . Continual reflections of these waves, from both ends of the line, subsequently build up a standing-

wave steady state, in which the volume energy of electric flux is different from, and ordinarily much greater than that of the magnetic flux, at any one point in the dielectric. The transmission process retains, however, the same general character, the effect being one of summation of travelling waves and wave energies.

## BIBLIOGRAPHY

*without pretensions as to completeness.*

1. O. Heaviside. Reprinted Electrical Papers. London, 1892.
2. O. Heaviside. Electromagnetic Theory. London, 1893.
3. J. J. Thomson. Notes on Recent Researches in Electricity and Magnetism. Oxford, 1893.
4. A. G. Webster. The Theory of Electricity and Magnetism. London, 1897.
5. A. E. Kennelly. On the Mechanism of Electric Power Transmission. *Electrical World*, New York, Oct. 4, 1903, Vol. 42, p. 672.
6. A. E. Kennelly. The Process of Building up the Voltage and Current in a Long Alternating-Current Circuit. *Proc. Am. Ac. A. and Sc.*, Vol. XIII., No. 27, May, 1907, pp. 701-715.
7. A. E. Kennelly and S. E. Whiting. The Measurement of Rotary Speeds of Dynamo Machines by the Stroboscopic Fork. *Trans. A. I. E. E.*, Vol. 27, Part 1, pp. 631-646, July, 1908.
8. K. W. Wagner. Electromagnetische Ausgleichvorgänge in Freileitungen und Kabeln. Leipzig, 1908.
9. C. P. Steinmetz. Transient Electric Phenomena and Oscillations. New York, 1909.
10. E. Breisig. Theoretische Telegraphie. Braunschweig, 1910.
11. J. A. Fleming. The Propagation of Electrical Currents in Telephone and Telegraph Conductors. London, 1911.
12. C. P. Steinmetz. Electric Discharges, Waves and Impulses. New York, 1911.
13. A. E. Kennelly. The Application of Hyperbolic Functions to Electrical Engineering Problems. London, 1912.
14. W. Peterson. Über Wanderwellen Schutzeinrichtungen. *Archiv für Elektrotechnik*, Vol. 1, Part 6, pp. 233-254, 1912.
15. H. M. Pleijel. Om beräkning af ofverspanningar. *Teknik Tid. Elektroteknik*, 1st April, 1914.
16. L. Binder. Ueber Einschaltvorgänge und elektrischen Wanderwellen. *Elek. Zeit.*, 12th Feb., 1914.
17. W. O. Schumann. Beiträge zur der Frage Wellenformen und Deformationen bei Ausgleichvorgängen langs gestreckter Leiter. *Elek. Masch.*, 26th April, 1914.
- 17a. R. D. Huxley. Design for Artificial Transmission Line. *Elec. World*, May 2, 1914, p. 980.
18. R. Rudenberg. Entstehung und Verlauf elektrischer Sprungwellen. *Elek. und Masch*, 6th Sept., 1914.

19. A. Fraenckel. Theorie der Wechselströme. Berlin, 1914.
20. K. W. Wagner. Reflexion und Brechnung von Wanderwellen. *Archiv für Elektrotechnik*, Vol. II., 1914.
21. A. E. Kennelly. Chart Atlas of Complex Hyperbolic and Circular Functions. Harvard University Press, 1914.
22. A. E. Kennelly. Tables of Complex Hyperbolic and Circular Functions. Harvard University Press, 1914.
23. A. E. Kennelly. The Impedances, Angular Velocities and Frequencies of oscillating-Current Circuits. *Proc. I. R. E.*, August–November, 1915, pp. 1–32.
24. W. S. Franklin and B. MacNutt. Advanced Electricity and Magnetism. New York, 1915.
25. C. E. Magnusson and S. R. Burbank. An Artificial Transmission Line with Adjustable Line Constants. *Trans. A. I. E. E.*, Vol. XXXV., pp. 1245–1257, 1916.
26. K. W. Wagner. Ueber eine Formel von Heaviside zur Berechnung von Einschaltvorgängen. *Archiv für Elektrotechnik*, Vol. IV.
27. L. Binder. Wanderwellen an Freileitungen und in Kabeln. *Elek. Zeit.*, 27th July, 1917.
28. A. Benischke. Ueberspannungen in der Entwicklung der Hochspannungstechnik. *Elek. und Masch.*, 23rd Dec., 1917.
29. C. P. Steinmetz. Theory and Calculation of Electric Circuits. New York, 1917.
30. A. E. Kennelly. Artificial Electric Lines. New York, 1917.
31. H. W. Malcolm. The Theory of the Submarine Telegraph and Telephone Cable. London, 1917.
32. J. Biermanns. Ueber Wanderwellen Schutzeinrichtungen. *Archiv für Elektrotechnik*, Vol. 5, Part 7, pp. 215–237, 1917.
33. H. M. Pleijel. Vandringsvagor och deras formforandringar under fortplantning utefter ledningar. *Teknik Tid. Elektroteknik*, 6th Nov., 1918.
34. W. Rogowski. Spulen und Wanderwellen. *Archiv für Elek.*, Vol. VI.
35. F. E. Pernot. Electrical Phenomena in Parallel Conductors. Boston, 1918.
36. U. Nabeshima. Transient Electric Phenomena in Artificial Transmission Lines. A thesis towards the Degree of M.S. at the Mass. Inst. of Technology, Cambridge, Mass., 1919.
37. J. R. Carson. Theory of the Transient Oscillations of Electrical Networks and Transmission Systems. *Proc. A. I. E. E.*, Feb. 21, 1919, pp. 407–489.
38. T. G. Fry. The Solution of Circuit Problems. *Physical Review*, Aug., 1919, Vol. 14, No. 2.
39. A. E. Kennelly, R. N. Hunter and A. A. Prior. Oscillographs and their Tests. *Proc. A. I. E. E.*, Feb., 1920.
40. G. W. Pierce. Electric Oscillation and Electric Waves. New York, 1920.

LIST OF SYMBOLS EMPLOYED.

|                                       |  |                                   |
|---------------------------------------|--|-----------------------------------|
| $\alpha$                              | Linear hyperbolic angle or propagation constant of a uniform line  | (hyps/wire km.).                  |
| $B = C\omega$                         | Total susceptance of a line  | (mhos).                           |
| $b = c\omega$                         | Linear susceptance of a line.  | (mhos/w. km.).                    |
| $B_e$                                 | Electric flux density in a dielectric (statgausses, or $\kappa$ x statvolts/cm.).                              |                                   |
| $B_m$                                 | Magnetic flux density in a dielectric (gausses, or $\mu$ gilberts/cm.).  |                                   |
| $\beta^\circ$                         | Phase angle of lag   | (circular degrees).               |
| $C$                                   | Total capacitance of a line  | (farads).                         |
| $c$                                   | Linear capacitance of a line   | (farads/w. km.).                  |
| $\delta_A, \delta_B, \delta_P$        | Position angles at sending end, receiving end, and intermediate point on a line, in the steady state           | (hyps $\angle$ ).                 |
| $dx$                                  | Small element of line length   | (km.).                            |
| $E_A, E_B, E_{Am}$                    | Max. cyclic voltage at sending end and at receiving end of a line, in the steady state; also scalar max. value | (volts $\angle$ ).                |
| $E_{Pk}, E_{P\infty}$                 | Transitory voltage at point $P$ after the $k$ th reflection from $B$ and in the steady state                   | (volts).                          |
| $e, e_r, e_s$                         | Instantaneous voltage generally, at receiving end, at sending end  | (volts).                          |
| $e = 2.718\dots$                      | Napierian base   | (numeric).                        |
| $f$                                   | Impressed frequency  | (cycles per sec.).                |
| $G$                                   | Total leakance of a line   | (mhos).                           |
| $g$                                   | Linear leakance of a line  | (mhos/w. km.).                    |
| $\theta = \theta_1 + j\theta_2$       | Hyperbolic angle of a line and its components  | (hyps $\angle$ ).                 |
| $\theta' = \theta_1' + j\theta_2'$    | Angular distance of a point on a line from $A$ , the sending end   | (hyps $\angle$ ).                 |
| $\theta'' = \theta_1'' + j\theta_2''$ | Angular distance of a point on a line from $B$ the receiving end   | (hyps $\angle$ ).                 |
| $I_A, I_s$                            | Current at sending end of the line   | (max. cy. amperes $\angle$ ).     |
| $I_B, I_r$                            | Current at receiving end of the line   | (max. cy. amperes $\angle$ ).     |
| $I_0$                                 | Initial outgoing current at $A$  | (max. cy. amperes $\angle$ ).     |
| $I_{Pk}, I_{P\infty}$                 | Transitory current at point $P$ after the $k$ th reflection from $B$ , and in the steady state                 | (amperes $\angle$ ).              |
| $i, i_r, i_s$                         | Instantaneous current generally, at receiving end, at sending end  | (amperes $\angle$ ).              |
| $j = \sqrt{-1}$                       |  |                                   |
| $k$                                   | Number of arrival wave, or of a $B$ reflected wave, at a point $P$   | (numeric).                        |
| $\kappa$                              | Electric inductivity of a dielectric   | (statgausses/statsvolts-per-cm.). |
| $\mathcal{L}$                         | Total inductance of a line   | (henrys).                         |
| $L$                                   | Length of a line   | (km.).                            |
| $l$                                   | Linear inductance of a line  | (henrys/w. km.).                  |
| $\lambda$                             | Wave length on a line  | (km.).                            |

|                          |  |                             |
|--------------------------|--|-----------------------------|
| $m$                      | Vector voltage transmission coefficient at junction  | (numeric $\angle$ ).        |
| $\mu$                    | Magnetic permeability  | (gausses/gilberts-per-cm.). |
| $n$                      | Vector current transmission coefficient  | (numeric $\angle$ ).        |
|                          | also the number of single wave passages over a line per second                                   | (numeric/sec.)              |
| $P = P_e + P_m$          | Total average power at sending end of a line in transient state                                  | (watts).                    |
| $P_e, P_m$               | Average power of transmitting electric flux and magnetic flux along line, at $A$                 | (watts).                    |
| $\pi = 3.1415 \dots$     |  | (numeric).                  |
| $R$                      | Total resistance of a line   | (ohms).                     |
| $r$                      | Linear resistance of a line  | (ohms/w. km.).              |
| $\sigma$                 | Impedance of load at $B$   | (ohms $\angle$ ).           |
| $T$                      | Time of transit of waves along line from $A$ to $B$ , or $B$ to $A$                              | (seconds).                  |
| $T_1$                    | Time of transit of waves along line from $A$ to $P$  | (seconds).                  |
| $T_{P1}, T_{P2}, T_{Pk}$ | Time of transit of first, of second and of $k$ th wave reflection from $B$ to $P$                | (seconds).                  |
| $t$                      | Time elapsed from switchclosure at $A$   | (seconds).                  |
| $v$                      | Velocity of propagation of waves along line  | (km./sec.).                 |
| $w, w_k$                 | Growth coefficient of waves at point $P$ in transient state, coefficient after $k$ th reflection | (numeric $\angle$ ).        |
| $w_e, w_m$               | Volume energy in dielectric of electric flux and of magnetic flux                                | (ergs/c.c.).                |
| $X = \mathcal{L}\omega$  | Total reactance of line  | (ohms).                     |
| $x$                      | Linear reactance of line   | (ohms/w. km.).              |
| $Y$                      | Total admittance of line   | (mhos $\angle$ ).           |
| $Z$                      | Total impedance of line  | (ohms $\angle$ ).           |
| $z_0$                    | Surge impedance of line  | (ohms $\angle$ ).           |
| $Z_{P1}, Z_{Pa}$         | Impedance at and beyond a point in a line after $k$ th reflection from $B$ , and in steady state | (ohms $\angle$ ).           |
| $\omega$                 | Impressed angular velocity   | (radians/sec.).             |
| logh                     | Hyperbolic logarithm, or logarithm to Napierian base.  |                             |
| hyp                      | Hyperbolic radian.   |                             |
| w. km.                   | Wire kilometer.  |                             |
| r.m.s.                   | Root mean square.  |                             |
| $ E $                    | Size of complex $E$ .  |                             |